BBA - Molecular Basis of Disease 1865 (2019) 708–723

Contents lists available at ScienceDirect

BBA - Molecular Basis of Disease

journal homepage: www.elsevier.com/locate/bbadis

Down-regulated expression of LINC00518 prevents epithelial cell growth and metastasis in breast cancer through the inhibition of CDX2 methylation and the Wnt signaling pathway

Hong-Bin Wang[a,1], Hong Wei[b,1], Jin-Song Wang[a], Lin Li[a], An-Yue Chen[a], Zhi-Gao Li[a,*]

[a] Department of Breast Surgery (No. 2 Sickroom), Harbin Medical University Cancer Hospital, Harbin 150081, PR China
[b] Department of In-Patient Ultrasound, The 2nd Affiliated Hospital of Harbin Medical University, Harbin 150081, PR China

ARTICLE INFO

Keywords:
Long intergenic non-protein coding RNA
LINC00518
CDX2
Methylation
Wnt signaling pathway
Breast cancer epithelial cells

ABSTRACT

Breast cancer (BC)-related mortality is associated with the potential metastatic properties of the primary breast tumors. The following study was conducted with the main focus on the effect of LINC00518 on the growth and metastasis of BC epithelial cells *via* the Wnt signaling pathway through regulation of the methylation of CDX2 gene. Initially, differentially expressed long intergenic non-protein coding RNAs (lincRNAs) related to BC were screened out in the Cancer Genome Atlas (TCGA) database, after which we detected the LINC00518 expression and localization in BC tissues and cells. Then the CDX2 positive expression and methylation level were identified. The targeting relationship of LINC00518 and CDX2, and binding methyltransferase in the promoter region were examined. BC epithelial cell proliferation, colony formation ability, invasion, migration and apoptosis were further evaluated. The lincRNA expression data related to BC downloaded from the TCGA database revealed that there was a high expression of LINC00518 in BC, and a negative correlation between LINC00518 and CDX2. In addition, LINC00518 promotes CDX2 methylation by recruiting DNA methyltransferase through activating the Wnt signaling pathway. The down-regulation of LINC00518 inhibited proliferation, invasion, migration, and EMT of BC epithelial cells while enhancing apoptosis. The inhibitory effects of LINC00518 down-regulation was reversed by CDX2 down-regulation. In conclusion, our findings revealed that down-regulation of LINC00518 might have the ability to suppress BC progression by up-regulating CDX2 expression through the reduction of methylation and blockade of the Wnt signaling pathway, resulting in the inhibition of proliferation and promotion of apoptosis of BC epithelial cells.

1. Introduction

Breast cancer (BC) ranks as the most frequently occurring cancer among females and the second most common cancer worldwide [1]. BC is the main cause of cancer-related mortality in women worldwide [2]. In 2012, reports showed that BC accounted for 521,900 deaths and that there were about 1.7 million newly diagnosed patients in the same year [3]. BC is characterized by distinct pathological and clinical features with intratumoral and intratumoral heterogeneity [4]; the treatment and prognosis of BC is significantly affected by these clinicopathological factors, which include tumor size, tumor stage and progesterone receptor [5]. During the early stages of BC metastasis, epithelial cells tend to penetrate the basement membrane and then invade surrounding stroma, where the paracrine signaling between the fibroblasts and epithelial tumor cells leads to the metastatic cascade [6]. Invasion and metastasis are the final and fatal stages of cancer progression in BC, and there is a limitation regarding the therapeutic options for metastatic BC [7]. Although neoadjuvant and systemic chemotherapy provides the alleviation of the effects and symptoms of BC patients, potential therapeutic molecular targets are highly required, particularly for cases where there is metastasis [8].

Long intergenic noncoding RNAs (lincRNAs) have been highlighted as new regulatory molecules characterized by cell-type specific expression and subcellular compartment localization [9]. LincRNAs play a critical role in the pathogenesis and development of BC by interacting with cancer related genes [10,11]. Long intergenic non-protein coding RNA 518 (LINC00518), with the chromosomal location in 6p24.3, which is close to the 6p25 region, has common copy number gains in

* Corresponding author at: Department of Breast Surgery (No. 2 Sickroom), Harbin Medical University Cancer Hospital, No. 150, Haping Road, Nangang District, Harbin 150081, Heilongjiang Province, PR China.
E-mail address: lizhigao_drlzg@163.com (Z.-G. Li).
[1] These authors contributed equally to this work.

https://doi.org/10.1016/j.bbadis.2019.01.003
Received 24 August 2018; Received in revised form 7 December 2018; Accepted 2 January 2019
Available online 04 January 2019
0925-4439/

melanoma [12]. In BC, there is a significant increase in LINC00518 expression and silencing of this molecule could result in enhanced anti-tumor effect of Adriamycin [13]. The findings from this study found that CDX2 was a target gene of LINC00518, and the overexpression of LINC00518 could potentially promote CDX2 methylation. A prior study has demonstrated that CDX2 polymorphism may serve as an underlying biomarker for vitamin D treatment in BC [14]. Caudal-related homeobox 2 (CDX2), located in the nuclei of mucous epithelial cells in the intestine, participates in the development, proliferation and differentiation of epithelial cells [15]. CDX2 has previously been identified as a tumor suppressor in adult colon, and its low expression has been linked with poor overall survival rate [16]. Another interesting discovery found that the Wnt signaling pathway modulates many aspects of vertebrate development and its dysregulation results in several kinds of developmental defects and diseases including cancer [17]. An abnormality in the Wnt signaling pathway is known to enhance the development of triple-negative BC [18]. Blockade of the Wnt signaling results in the suppression of BC metastasis by inhibiting cancer stem cell-like phenotype which is the main factor associated with the heterogeneity observed in BC [19]. HER2 promotes proliferation and migration of HER2 positive BC cells through the Wnt signaling pathway [20]. Therefore, the aforementioned findings are all suggestive of the important role Wnt signaling pathway plays in the progression of BC. However, more studies are required to elucidate the specific mechanism of Wnt signaling pathway in the regulation of BC progression. Recently, a number of studies reported that tumor suppressor CDX2 inhibits the Wnt signaling pathway [21,22]. Since the high expression of LINC00518 in BC has been previously demonstrated, we conducted the following study to further explore and examine the hypothesis that LINC00518 activates the Wnt signaling pathway by inhibiting the target gene CDX2.

2. Materials and methods

2.1. Ethics statement

This study had been approved by the Ethics Committee of Harbin Medical University Cancer Hospital. All participating patients signed informed consent. All animal procedures were conducted in accordance with the National Institutes of Health Guide for the Care and Use of Laboratory Animals (National Institutes of Health, Bethesda, MA, USA). The animals received humane care based on the guideline of Guidebook for the Care and Use of Laboratory Animals.

2.2. Bioinformatics analysis

The lincRNA expression data of BC was downloaded from the Cancer Genome Atlas (TCGA) (http://cancergenome.nih.gov/) database, and the statistical analysis was performed with the R software. Differential analysis was carried out for the transcriptome profiling data with package edgeR of the R software [23]. False positive discovery (FDR) correction was adopted on *p*-value with package multi-test. Differentially expressed genes (DEGs) were screened out with FDR < 0.05 and $|\log2foldchange| > 2$ set as the threshold.

2.3. Study subjects

A total of 60 surgically resected cases of BC tissues along with adjacent normal tissues (as the control) were collected from Harbin Medical University Cancer Hospital between April 2014 and August 2017. There were 43 cases below the age of 50 years old, and 17 cases over the age of 50 years old. The inclusion criteria included the following: patients who hadn't received chemotherapy or radiotherapy prior to the operation, patients who had never taken hormone drugs and patients whose BC diagnosis had been pathologically confirmed as nonspecific invasive BC. All cases were observed for morphological changes and diagnosed by more than two associate chief physicians according to the World Health Organization (WHO) classification standard [24]. There were 37 cases in stage I + II and 23 cases in stage III. The standard of tumor staging was carried out according to the 6th edition of American Joint Committee on Cancer (AJCC) Tumor-Node-Metastasis (TNM) staging system [25]. Based on this staging system, there were 44 cases in stage I + II, 16 cases in stage III a, and no lymph node metastasis in all cases. Afterwards, all specimens were fixed with 10% formaldehyde, dehydrated conventionally, embedded in paraffin, and sliced at a thickness of 4 μm.

2.4. Immunohistochemistry

The tumor tissues of nude mice were embedded with paraffin, sliced, dewaxed, and dehydrated, followed by antigen repair in a water bath. Next, the tissue sections were added with normal goat serum sealing solution (C-0005, Shanghai Haoran Biotechnology Co., Ltd., Shanghai, China), and allowed to stand at room temperature for 20 min, followed by the addition of the primary antibody, rabbit anti-human CDX2 (ab88129, 1:100, Abcam Inc., Cambridge, MA, USA) for culture overnight at 4 °C. The secondary antibody, goat anti-rabbit immunoglobulin G (IgG; 1: 1000, ab6785, Abcam Inc., Cambridge, MA, USA) was then added for a 20-min culture at 37 °C. The horseradish peroxidase (HRP)-labeled streptomycin albumen protein working solution (0343-10000U, Imunbio Biotechnology Co., Ltd., Beijing, China) was added for 20-min culture at 37 °C. The sections were colored by diaminobenzidine (DAB; ST033, Guangzhou Whiga Technology Co., Ltd., Guangzhou, Guangdong, China), counter-stained with hematoxylin (PT001, Shanghai Bogoo Biological Technology Co., Ltd., Shanghai, China) for 1 min, washed, after which 1% ammonia water was added to facilitate a change of color to blue. After washing, the sections were mounted with neutral gum, observed and photographed under a microscope. Next, 5 high-power fields were randomly selected from each section with 100 cells per field. The number of positive cells $< 10\%$ was regarded as negative, the number of positive cells $> 10\%$ and $< 50\%$ as positive, and the positive cell number $> 50\%$ as strong positive [26].

2.5. Bisulfite sequencing polymerase chain reaction (BSP)

The frozen BC tissues and adjacent normal tissues that were stored previously were collected, out of which 50 mg was cut off, and 300 μL of peripheral blood was extracted. DNA was extracted according to instructions of the Dneasy Blood & Tissue Kit, and the purity and content of DNA were measured by an ultraviolet spectrophotometer. Next, 2 μg genomic DNA was modified with the use of hydrosulfite according to EpiTect® Bisulfite Handbook. The hydrosulfite-modified DNA was used as a template for PCR amplification reaction. The CDX2 BSP primer sequences are shown in Table 1. The reaction conditions were as follows: pre-denaturation at 95 °C for 15 min; 50 circles of denaturation at 95 °C for 30 s, annealing at 57 °C for 30 s, and extension at 72 °C for 20 s. Afterwards, 5 μL of PCR amplified products was used for 2.5% agarose gel electrophoresis and observed on a gel image imager. Additional 20 μL of PCR product was purified by the QIAquick purification kit and sent to Shanghai Langkang Biotechnology Co., Ltd. (Shanghai, China) for sequencing, the results of which were analyzed by the CpG viewer software. This method was also applicable for cells.

2.6. Methylation specific polymerase chain reaction (MSP)

The frozen BC tissues and adjacent normal tissues that had been stored previously were taken and DNA was extracted by the ammonia chloroform extraction method and modified by sodium bisulfite. The modified DNA was purified by a DNA purification kit (Promega Corporation, Madison, WI, USA). The hydrosulfite modified DNA was used as a template for amplification. The primer sequences of CDX2

Table 1
Primer sequence for RT-qPCR.

Gene	Forward sequence (5′-3′)	Reverse sequence (5′-3′)
BSP-CDX2	TTGGAAAATAGGGATAATTAGTTAG	AACTAAAACTCCAACCTATATCTTC
MSP-M	ATTTTAGAAATGATAGGATGAAGGC	GAACTAAACAACCTAACTCGACGAC
MSP-U	TTTTAGAAATGATAGGATGAAGGTGA	CAAACTAAACAACCTAACTCAACAA
LINC00518	AGAGTCCTCTCTCTCGGCAT	AACCCCTTTGATCCTCAGCG
CDX2	CCACGCTGGGGCTCTCT	GTCTAGCAGAGTCCACGCTC
β-catenin	CTGCAGGGGTCCTCTGTG	TGCATATGTCGCCACACC
c-Myc	CCCAGCGAGGATCATCTGGAAGAA	GAGAGCCGCTCCACATAGCAGTC
CyclinD1	TACCCCAATAATCAACTCG	GATTGCCTAGAACCCCAC
GSK3β	GGCAGCATGAAAGTTAGCAGA	GGCGACCAGTTCTCCTGAATC
Slug	AAGCATTTCAACGCCTCCAAA	GGATCTCTGGTTGTGGTATGACA
Snail1	TCGGAAGCCTAACTACAGCGA	AGATGAGCATTGGCAGCGAG
Twist1	CGACGACAGCCTGAGCAACA	CCACAGCCCGCAGACTTCTT
ZEB1	GATGATGAATGCGAGTCAGATGC	ACAGCAGTGTCTTGTTGTTG
ZEB2	GACAGATCAGCACCAAATGC	GTAAGGTTTTTCACCATGTG
E-cadherin	CTGAGAACGAGGCTAACG	GTCCACCATCATCATTCAATAT
β-actin	TGGTGGGTATGGGTCAGAAGGACTC	CATGGCTGGGGTGTTGAAGGTCTCA

Note: RT-qPCR, reverse transcription quantitative polymerase chain reaction; BSP, Bisulfite sequencing polymerase chain reaction; CDX2, Caudal-related homeobox 2; MSP, Methylation specific polymerase chain reaction; LINC00518, long intergenic non-protein coding RNA 518; GSK3β, Glycogen synthase kinase 3beta; ZEB, Zinc finger E-box binding homeobox transcription factor.

MSP-M and CDX2 MSP-U were synthesized by Shanghai Sangon Biotechnology Co., Ltd. (Shanghai, China) (Table 1). The reaction condition was as follows: pre-denaturation at 95 °C for 10 min; 35 circles of denaturation at 95 °C for 1 min, annealing at 60 °C for 50 s, and extension at 72 °C for 10 min. The results were then classified as follows [27]: those that can amplify the products using methylation primers, and non-methylation primers cannot amplify products while these results were on the contrary in the case of exhaustive methylation, and the complete non-methylation; in cases were both can amplify the product was regarded as partial methylation. This method was also applicable for cells.

2.7. Reverse transcription quantitative polymerase chain reaction (RT-qPCR)

Total RNA of BC and adjacent normal tissues were extracted by the TRIZOL kit (15596–018, Beijing Solarbio Science & Technology Co., Ltd., Beijing, China). The primers used in this study were synthesized by Takara (Takara Inc., Dalian, Liaoning, China) (Table 1). The reverse transcription was conducted in accordance with the instructions of the cDNA reverse transcription kit (Beijing Ya'anda Biological Technology Co., Ltd., Beijing, China). The reaction conditions were set at 42 °C for 30–50 min (reverse transcription reaction) and 85 °C for 5 s (reverse transcriptase inactivation reaction). The PCR condition was as follows: pre-denaturation at 95 °C for 4 min; 30 circles of denaturation at 95 °C for 30 s, annealing at 57 °C for 30 s, and extension at 72 °C for 30 s. With β-actin as internal reference primers, the relative transcriptional levels of the target genes were calculated using the $2^{-\Delta\Delta Ct}$ method [28]. This method was also suitable for cells. Following cell transfection for 48 h, the cytoplasm protein extraction buffer and the nuclear protein extraction buffer were separately used for the separation of the cytoplasm and nucleus, and the subsequent experiments were carried out.

2.8. Western blot analysis

Total protein of BC and adjacent normal tissues and cells were extracted. The protein concentration was determined with the use of a bicinchoninic acid (BCA) kit (20201ES76, Yeasen Biotechnology Co., Ltd., Shanghai, China). Next, the concentration of protein was quantified and separated by polyacrylamide gel electrophoresis (PAGE), transferred to the polyvinylidene fluoride (PVDF) membrane by the wet transformation method, and sealed in 5% bovine serum albumin (BSA) for 1 h. The membrane was incubated at 4 °C overnight with the addition of the following primary antibodies: rabbit anti-human antibodies to CDX2 (ab88129, 1:2000), β-catenin (ab16051, 1:500), c-Myc (ab39688, 1:800), CyclinD1 (ab226977, 1:2000), Glycogen synthase kinase 3beta (GSK3β; ab32391, 1:7000), Slug (ab106077, 1:2000), Snail1 (ab82846, 1:300), Twist1 (ab50581, 1:2000), Zinc finger *E*-box binding homeobox transcription factor (ZEB)1 (ab124512, 1:3000), ZEB2 (ab138222, 1:800) and E-cadherin (ab15148, 1:500). The membrane was washed 3 times with Tris-Buffered Saline Tween-20 (TBST), 5 min each time, and added with HRP-labeled goat anti-rabbit IgG (ab205718, 1: 20000) at room temperature for 1 h. All antibodies were purchased from Abcam Inc. (Cambridge, MA, USA). The membrane was developed following three cycles of TBST washes, 5 min each time. The ImageJ 1.48u software (National Institutes of Health, Bethesda, MA, USA) was used for protein quantitative analysis, which was carried out based on the gray value of the target band to glyceraldehyde-3-phosphate dehydrogenase (GAPDH). This method was also suitable for cells. After 48-h cell transfection and culture, the segmentation of nucleus and cytoplasm was performed.

2.9. Cell treatment

Human normal breast epithelial cell line HBL-100 and human BC epithelial cell lines MCF-7, MDA-MB-231 and MDA-MB-4359 [29] were purchased from the Typical Culture Preservation Commission Cell Bank of Chinese Academy of Sciences (Shanghai, China). Cells were cultured in Dulbecco's modified Eagle's medium (DMEM) containing 10% calf serum, and penicillin-streptomycin mixture at the ratio of 1:1 was added into the culture medium, and 100 U/mL was used as the final concentration. Subsequently, the cells were cultured in a 5% CO_2 incubator at 37 °C, treated with 0.25% trypsin and seeded in a 6-well plate at a density of 3×10^5 cells/well. RT-qPCR was conducted when cell confluence reached 70% ~ 80% in order to measure the LINC00518 expression in each cell line. The cell line with the highest LINC00518 expression at growth logarithmic phase was used for subsequent experiments.

2.10. Cell transfection and grouping

MCF-7 cells at logarithmic growth phase were inoculated into a 6-well plate at a density of 4×10^5 cells/well. The LINC00518 shRNA sequence (Santa Cruz Biotechnology, Inc., Santa Cruz, CA, USA) diluted by 50 μL of Royal Park Memorial Institute (RPMI) 1640 culture solution, was fully mixed with the X-tremeGENE siRNA transfection reagent diluted by 50 μL of RPMI 1640 culture solution at the ratio of 2.5 μL: 0.5 μg of siRNA, and then added to the 6-well plate after 20-min of

standing. The plasmids were transfected into cells according to lipofectamine 2000 instructions (Invitrogen, Carlsbad, CA, USA). A total of 250 μL of serum-free medium Opti-MEM (Gibco, Grand Island, N.Y., USA) was used to dilute 100 pmol vector (the final concentration was 50 nM), mixed evenly and incubated at room temperature for 5 min. Next, 250 μL of serum-free medium Opti-MEM was applied to dilute 5 μL of lipofectamine 2000, after which it was mixed and incubated at room temperature for 5 min. The two mixtures were mixed, then incubated at room temperature for 20 min and added into culture wells. After transfection, cells were cultured in a 5% CO_2 incubator at 37 °C with saturated humidity. After 48 h, the culture medium containing the transfection solution was replaced with the RPMI 1640 culture medium (Santa Cruz Biotechnology, Inc., Santa Cruz, CA, USA) containing 10% fetal bovine serum (FBS), followed by further 24–48 h culture, which was used for subsequent experiments.

BC cells were assigned into: oe-LINC00518 NC group (transfected with LINC00518 NC plasmid), oe-LINC00518 group (transfected with LINC00518 overexpression plasmid), sh-LINC00518 NC group (transfected with sh-LINC00518 NC plasmid), sh-LINC00518 group (transfected with sh-LINC00518 plasmid), oe-LINC00518 + dimethyl sulphoxide (DMSO) group (transfected with LINC00518 overexpression plasmid and DMSO, the 5-AZA-2′-deoxycytidine (5-AZA-CdR) dissolved liquid), oe-LINC00518 + 5-Aza-CdR group (transfected with LINC00518 overexpression plasmid and DNA methylation inhibitor 5-AZA-CdR), oe-CDX2 NC group (transfected with CDX2 NC plasmid), and oe-CDX2 group (transfected with CDX2 overexpression plasmid). The transfection sequence and plasmids were constructed by Shanghai Sangon Biotechnology Co., Ltd. (Shanghai, China). Overexpression vector was pGC-FU-GFP, and knockdown vector was pLVX-shRNA. After transfection for 48 h, the cells were observed under a fluorescence microscope to verify whether the transfection was successful [30]. The fluorescence reaction of the same cell picture under the fluorescence and non-fluorescent conditions was compared. The successful transfection in the fluorescent condition showed green fluorescence, and the fluorescence did not display in the non-fluorescent field.

2.11. T cell factor optimal promoter (TOPflash) reporter assay

After transfection for 48 h, MCF-7 cells were collected and lysed, and 40 μL of lysate was absorbed. The fluorescence of 20 μL of firefly luciferase substrate or the renilla luciferase substrate (as the internal reference) was added, and the time of each lysate needed to be consistent with the substrate. The firefly luciferase value and the renilla luciferase value in each well were measured by a spectrophotometer, using the following formula: Relative luciferase units (RLU value) = firefly luciferase value/renilla luciferase value, which suggested the activation level of transcription factors in the intracellular Wnt signaling pathway.

2.12. Fluorescence in situ hybridization (FISH)

LncRNA cell sub-location website http://lncatlas.crg.eu/ was used to predict the localization of LINC00518 expression in MCF-7 BC cells. Subcellular localization of LINC00518 was detected by the FISH Kit (F. Hoffmann-La Roche Ltd., Basel, Switzerland). Digoxin-labeled LINC00518 probe was purchased from Sigma (St. Louis, MO, USA). The antagonistic LINC00518 probe was used as NC and stained with 4′,6-diamidino-2-phenylindole (DAPI; Sigma, St. Louis, MO, USA) for 10 min. The kit was washed two times with cold phosphate buffer saline (PBS), and laser confocal scanning microscope was used to record fluorescence image.

2.13. Dual-luciferase reporter gene assay

The targeting effects of LINC00518 on CDX2 were analyzed by the biological prediction website (https://cm.jefferson.edu/rna22/Interactive/) and the dual-luciferase reporter gene assay. According to the binding sequence of promoter region of CDX2 mRNA and LINC00518, the target sequence and mutation sequence were designed. CDX2 promoter wild type (Wt) sequence was: GGCACAGGGGCTCACA CCTGTAATCCCAGCACTTTAGGAGGCTGAGGCAGGAGGATCACCTGAG CCCAGGATAGCAAGACCCTATCTCTACAAAAA; mutant (Mut) sequence was: CTGGTTATGCGATAACGGCACAGGGGCTCACATATCCTA AGCATCGTCGAAGCATTGAACGCCATTTGCCCGCGAAGAGCTGGTTAT GCGATAACG. The luciferase activity of the LINC00518 to the CDX2 promoter region was assessed according to the instructions of the Genecopoeia's dual-luciferase detection kit (Beijing Solarbio Science & Technology Co., Ltd., Beijing, China). The fluorescence intensity was examined by a GLomax20/20 Luminometer fluorescence detector of Promega Corporation (Madison, WI, USA).

2.14. RNA immunoprecipitation (RIP)

The cells were collected using a cell scrape, centrifuged at 402 *g* for 5 min at 4 °C, and the supernatant was discarded. RIP lysis buffer (N653-100 mL, Shanghai Haoran Biotechnology Co., Ltd., Shanghai, China) was added to obtain cell lysate. Each tube was added with 50 μL of magnetic beads and 0.5 mL of RIP Wash Buffer (EHJ-BVIS08102, Xiamen Huijia Biotechnology Co., Ltd., Xiamen, Fujian, China), after which the beads were collected and re-suspended with 100 μL of RIP Wash Buffer with the supernatant removed. Next, 5 μg of DNA methyltransferase (DNMT) antibody (P10502500, Shenzhen Otwo Biological Technology Co., Ltd., Shenzhen, Guangdong, China) was added, and incubated at room temperature for 30 min. The mixture of magnetic beads and antibody were added with 900 μL of RIP Immunoprecipitation Buffer (P10403138, Shenzhen Otwo Biological Technology Co., Ltd., Shenzhen, Guangdong, China), and 100 μL of supernatant was absorbed to the magnetic bead-antibody tube. With 1 mL as the final volume of the immunoprecipitation reaction, cells were incubated at 4 °C overnight while rotating, and added with 150 μL of proteinase K buffer and incubated at 55 °C for 30 min. RNA was purified, extracted by the TRIZOL method, and determined by RT-qPCR.

2.15. Chromatin immunoprecipitation (CHIP)

The CHIP kit (Millipore, Billerica, MA, USA) was used to study the enrichment of DNMT1, DNMT3a and DNMT3b in the promoter region of CDX2 gene. The cells were fixed at room temperature for 10 min so that DNA and protein were immobilized and cross-linked. After cross-linking, they were randomly broken into fragments of appropriate size following ultrasonic treatment. After centrifugation at 4 °C, the supernatant was collected supernatant and divided into three tubes, which were then added with positive control antibody to RNA polymerase II, NC antibody to IgG and target protein specific antibodies to DNMT1 (ab13537), DNMT3a (ab2850) and DNMT3b (ab2851) respectively, and incubated overnight at 4 °C. The target protein specific antibodies were all rabbit antibodies and purchased from Abcam (Cambridge, MA, USA). The endogenous DNA- protein complex was precipitated by Protein Agarose/Sepharose and de-cross-linked at 65 °C overnight. The phenol/chloroform was used to extract and purify DNA fragments. The binding of DNMT1, DNMT3a and DNMT3b to CDX2 promoter region was tested by specific primers of CDX2 gene promoter region (Table 1).

2.16. Cell counting kit-8 (CCK-8)

Cell proliferation was measured according to the instructions of the CCK-8 (GM-040101-5, Dojindo Molecular Technologies, Gaithersburg, MD, USA). Cells in logarithmic growth phase after transfection were treated with trypsin, and seeded into a 96-well plate at a density of 5×10^3 cells/μL and incubated in a 5% CO_2 incubator at 37 °C. Six duplicated wells were set in each group. Cells were continuously

cultured for 2 d, and 10 μL of CCK-8 solution was added to each well at the last 4 h. After continuous culture for 4 h, the optical density (OD) value was measured at a wavelength of 450 nm using a spectrophotometer (μV-1800A, Shanghai Macylab Instruments Inc., Shanghai, China). The number of living cells in different treatment groups was deduced according to the OD value, and the cell growth curve was depicted.

2.17. 5-ethynyl-2′-deoxyuridine (EdU) staining

A total of 5×10^4 cells was seeded in a 96-well plate. After 48-h culture, cells were detached, collected and incubated in the culture medium containing Edu for 2 h. After PBS washing, the cells were fixed with 4% paraformaldehyde for 30 min, and incubated with the addition of reagent B, C, D and E separately according to the instructions of the Edu kit (Guangzhou RiboBio Co., Ltd., Guangzhou, Guangdong, China). Afterwards the cells were washed with PBS, and incubated with Hoechst33342 staining solution for 30 min at room temperature. After PBS washing, cells were observed and photographed under a fluorescence microscope. The cells, whose nuclei were stained with red, were positive labeled cells. The number of positive and negative cells in any 3 visual fields was counted under the microscope. The rate of Edu labeling (%) = positive cell number/(number of positive cells + number of negative cells) × 100%.

2.18. Dual soft-agar colony formation assay

Cells in the logarithmic growth phase were adjusted to a density of 5×10^6 cells/mL by 0.3% surface glue, and added to the solidified base glue at 1.0 mL/well. Three duplicated wells were set for each group. Cells were incubated continuously in a 5% CO_2 incubator at 37 °C for 10–14 d, and culture medium was added properly to prevent drying. Cell colony formation was observed under a light microscope and colony formation rate was calculated using the following formula: Colony formation rate = colony forming number/seeded cell number × 100%.

2.19. Transwell assay

The transfected cells were diluted with 100 μL of serum-free medium and inoculated at a density of 1×10^6 cells/mL. The basolateral chamber was added with 500 μL of DMEM containing 20% FBS. Three duplicated wells were set in each group. Cells were incubated in a 5% CO_2 incubator at 37 °C for 24 h. Transwell chamber was washed 2 times with PBS, fixed with 5% glutaraldehyde at 4 °C, stained with 0.1% crystal violet for 5 min, and washed twice with PBS. The cotton balls were used to wipe off the surface cells. Then cells were observed under an inverted fluorescence microscope (Nikon Corporation, Tokyo, Japan). Next, 5 visual fields were photographed randomly, and the average number of cells passing through the chamber was obtained in each group.

2.20. Scratch test

The transfected cells were incubated in a 5% CO_2 incubator at 37 °C for 24 h, and a horizontal scratch was created in the single layer cells with a 10 μL pipette tip. After 3 washes with PBS, cells were added with serum-free medium, and incubated for 24 h, with the medium washed out. Cells were rinsed 3 times with PBS, and cell migration was observed at the 0th and 48th h under an inverted microscope. Three parts were selected in each group for photograph and the relative distance between the cells on both sides of the scratch was measured using the formula: relative migration distance of the cells = the distance difference/2. Cell relative migration rate = relative migration distance/the distance from the scratch edge to the scratch midline at the 0th h.

2.21. Terminal deoxynucleotidyl transferase (TdT)-mediated dUTP nick end labeling (TUNEL) assay

After 48-h transfection, the cells were collected and added with the mixture of TUNEL reaction (11684817910, Beijing Solarbio Science & Technology Co., Ltd., Beijing, China) for 30-min incubation in a wet box at 37 °C. TUNEL-peroxidase (POD) conversion agent (AP005, Shanghai 7 sea Biotechnology Co., Ltd., Shanghai, China) was added and incubated for 30 min in a wet box at 37 °C. Then cells were added with DAB substrate solution and allowed to stand at room temperature for 5–10 min, counter-stained with hematoxylin (PT001, Shanghai Bogoo Biological Technology Co., Ltd., Shanghai, China), sealed, and observed under a fluorescence microscopy to analyze the results, with the cells that appeared to have a green fluorescence were regarded as positive apoptotic cells. A total of 5 high-power fields were randomly selected to count the positive cells and total cells. The percentage of positive cells in the total number of cells was calculated as apoptotic index (AI). AI (%) = (apoptotic cells/total cells) × 100%.

2.22. Tumor xenografts in nude mice

BALB/c nude mice (aged 5–7 weeks and weighing 19–21 g; Shanghai Lingchang Biological Technology Co., Ltd., Shanghai, China) were fed at specific pathogen-free (SPF) grade environment. BALB/c nude mice were allocated into 6 groups (8 mice in each group) and inoculated with MCF-7 cells transfected with plasmids: oe-LINC00518 NC group, oe-LINC00518 group, sh-LINC00518 NC group, sh-LINC00518 group, oe-LINC00518 + oe-CDX2 NC group, and oe-LINC00518 + oe-CDX2 group.

The cells in the logarithmic growth phase were prepared for cell suspension with a density of 5×10^7 cells/mL, and 0.2 mL of cell suspension was inoculated to the subcutaneous layer of the left popliteal fossa of BALB/c nude mice using a 1 mL syringe. After inoculation, all nude mice were kept in the SPF grade animal house and raised in the laminar cover, and then the tumor growth was observed on the 7th, 14th, 21st and 28th d, and the data were recorded. The short diameter (a) and long diameter (b) of the tumor were recorded with a ruler, and the tumor volume = π (2ab)/6. The experiment was repeated 3 times. On the 28th d, the nude mice were euthanized and tumor was removed. The tumor tissues were fixed with 10% formaldehyde, routinely dehydrated, embedded paraffin and cut into 4 μm sections. Lymph node tissues were extracted and stained with hematoxylin and eosin to observe lymph node metastasis.

2.23. Statistical analysis

SPSS 19.0 statistical software (IBM Corp. Armonk, N.Y., USA) was used to analyze all statistical data. Measurement data with normal distribution were presented as mean ± standard deviation. The comparisons between two groups were analyzed by the *t*-test and the comparisons among multiple groups were conducted by one-way analysis of variance. Pairwise comparisons between groups were conducted using least significant difference test. Two-way analysis of variance was used to analyze the effects of two factors. $p < 0.05$ indicated a statistically significant difference.

3. Results

3.1. LINC00518 is predicted to be highly expressed in BC tissues and cells

There is a high expression in LINC00518 in BC and a negative correlation between LINC00518 and CDX2 (Fig. 1B) based on the lincRNA expression data related to BC that was downloaded from the TCGA database (Fig. 1A). LINC00518 expression was tested in 60 cases of BC tissues and adjacent normal tissues. The results of RT-qPCR showed that there was a significantly higher LINC00518 expression in

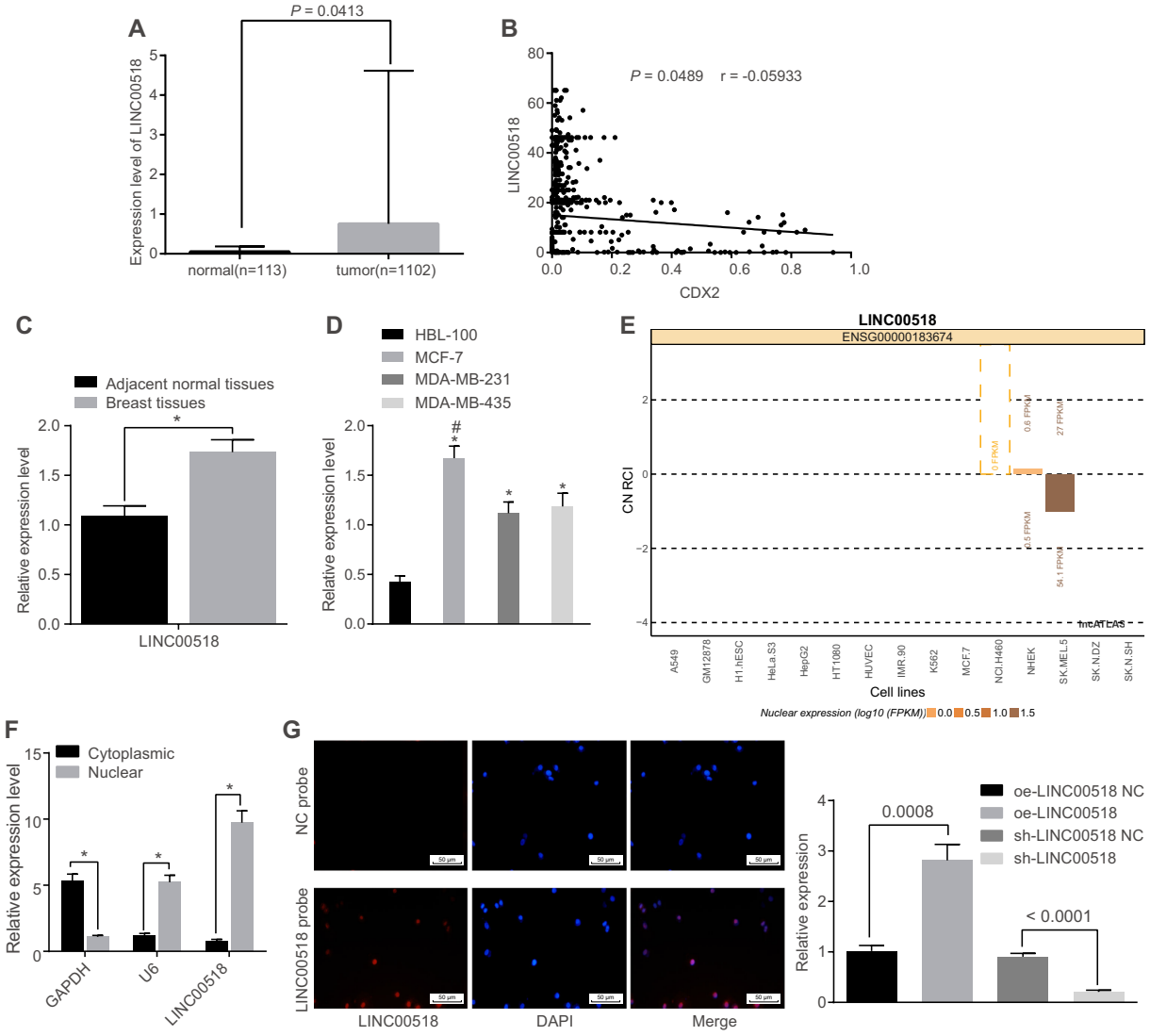

Fig. 1. There is a high expression in LINC00518 in BC tissues and cells. A, expression of LINC00518 in BC and normal tissues in the TCGA database; B, correlation analysis of LINC00518 and CDX2 in the TCGA database; C, LINC00518 expression in BC tissues and adjacent normal tissues was determined by RT-qPCR. The data were analyzed by *t*-test; D, LINC00518 expression in BC epithelial cell lines MCF-7, MDA-MB-231 and MDA-MB-435 measured by RT-qPCR. The data were analyzed by one-way ANOVA; E, the localization of LINC00518 in BC cell predicted by LncATLAS. The data were analyzed by *t*-test; F, the difference of LINC00518 expression in the nucleus and cytoplasm detected using nucleus and cytoplasm segmentation method; G, the localization of LINC00518 in BC cell verified using FISH (200×); H, LINC00518 overexpression and knockdown efficiency in MCF-7 cells tested by quantitative PCR; *, $p < 0.05$ *vs.* adjacent normal tissue or HBL-100 cell line or cytoplasm; # indicated the cell line with the highest LINC00518 expression; the statistical values are measurement data, sample size is 60, and the experiment was repeated 3 times; BC, breast cancer; TCGA, the Cancer Genome Atlas; LINC00518, long intergenic non-coding RNA 518; RT-qPCR, reverse transcription quantitative polymerase chain reaction; FISH, fluorescence *in situ* hybridization; GAPDH, glyceraldehyde-3-phosphate dehydrogenase; DAPI, 4′,6-diamidino-2-phenylindole; NC, negative control.

BC tissues than that in adjacent normal tissue ($p < 0.05$) (Fig. 1C). In order to study the effects of LINC00518 on BC epithelial cell lines, the BC epithelial cell lines with the highest LINC00518 expression were screened by RT-qPCR. The results showed that compared with the normal human breast epithelial cell line HBL-100, there was a high expression in LINC00518 in human BC epithelial cell lines MCF-7, MDA-MB-231 and MDA-MB-435, with the highest expression in MCF-7 cell line ($p < 0.05$). Therefore, the MCF-7 cell line was selected for the consequent experiments (Fig. 1D). The sub-cellular localization of LINC00518 was predicted by the LncATLAS site. The results showed that LINC00518 was located in the nucleus in multiple cell lines (Fig. 1E). The segmentation of nucleus and cytoplasm experiment was used for further verification and the result showed that there is a high expression in LINC00518 in nucleus ($p < 0.05$) (Fig. 1F). Finally, it was verified by FISH and results showed that LINC00518 expression was located in the nucleus (Fig. 1G). The results were all consistent with the prediction results of LncATLAS website. Quantitative PCR was used to examine the expression of LINC00518 in MCF-7 cells after LINC00518 knockdown or overexpression. The results showed that the transfection efficiency is appropriate for further experiments (Fig. 1H). These results indicated that LINC00518 was highly expressed in BC tissues and cells, and was located in nucleus.

3.2. LINC00518 down-regulation promotes BC epithelial cell apoptosis and inhibits cell proliferation, invasion and migration

Next, CCK-8, Edu staining, colony formation assay, TUNEL staining, Transwell assay and scratch test were conducted in order to explore the effects of LINC00518 overexpression and LINC00518 silencing on MCF-7 cell apoptosis, proliferation, invasion and migration. CCK-8 results

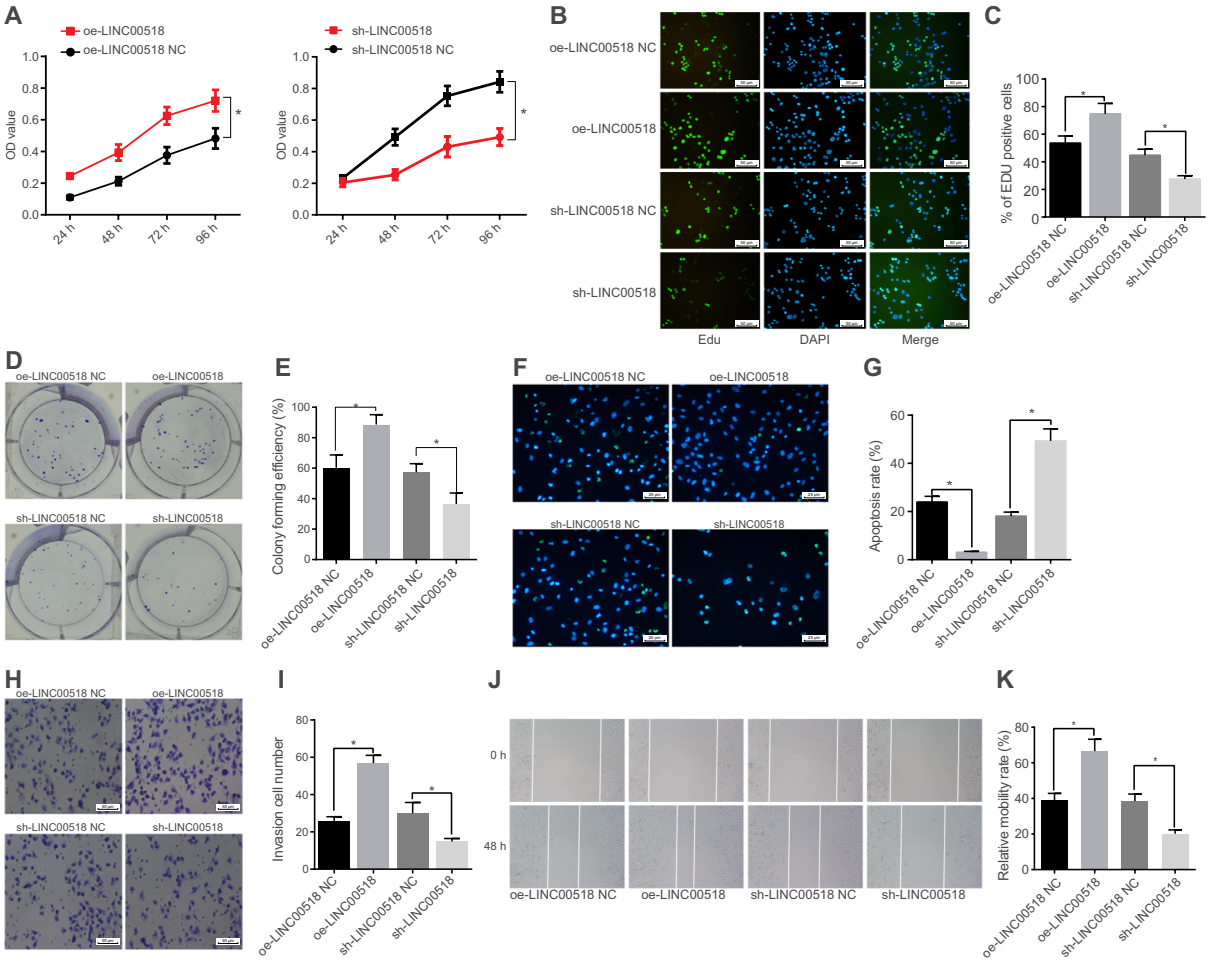

Fig. 2. Silencing of LINC00518 promotes epithelial cell apoptosis while inhibiting cell growth and proliferation, colony forming ability, invasion and migration in BC. A, OD value of BC epithelial cells detected by CCK-8; B, BC epithelial cell proliferation detected by EdU staining (200 ×); C, quantitative analysis for BC epithelial cell proliferation; D, colony formation of BC epithelial cells measured by dual soft-agar colony formation assay; E, quantitative analysis for BC epithelial cell colony formation ability; F, apoptosis conditions of BC epithelial cells detected by TUNEL staining (400 ×); G, quantitative analysis for apoptosis rate of BC epithelial cells; H, invasion ability of BC epithelial cells detected by Transwell assay (200 ×); I, quantitative analysis for BC epithelial cell invasion rate; J, the migration distance of BC epithelial cells detected by scratch test (100 ×); K, quantitative analysis for BC epithelial cell migration rate; *, $p < 0.05$ *vs.* the oe-LINC00518 NC group and the sh-LINC00518 NC group; the statistical values are measurement data, and the comparison among multiple groups was analyzed by one-way ANOVA; repeated-measures analysis of variance was adopted for comparison at different time points; the experiment was repeated 3 times; BC, breast cancer; LINC00518, long intergenic non-protein coding RNA 518; OD, optical value; CCK-8, Cell Counting Kit-8; Edu, 5-ethynyl-2′-deoxyuridine; TUNEL, Terminal deoxynucleotidyl transferase (TdT)-mediated dUTP nick end labeling; oe, overexpression; NC, negative control.

showed when the initial concentration was unchanged; there was no difference in the OD value at the 24th h in each group ($p > 0.05$). The oe-LINC00518 group increased the OD value of MCF-7 cells at the 48th h, 72nd h and 96th h significantly and the sh-LINC00518 group decreased the OD value at the 48th h, 72nd h and 96th h significantly, and inhibited cell proliferation ($p < 0.05$) (Fig. 2A). Edu results showed that red proliferative positive cells in the oe-LINC00518 group increased significantly, and decreased significantly in the sh-LINC00518 group ($p < 0.05$) (Fig. 2B–C). Colony formation assay results showed that the oe-LINC00518 group promoted colony formation and the sh-LINC00518 group inhibited colony formation ($p < 0.05$) (Fig. 2D–E). The results of TUNEL assay showed that the apoptotic cells were stained with green fluorescence, a decrease in cell apoptosis in the oe-LINC00518 group cell apoptosis, and enhanced apoptosis of MCF-7 cells in the sh-LINC00518 group ($p < 0.05$) (Fig. 2F–G). The results of Transwell assay indicated the invasion of MCF-7 cells was promoted in the oe-LINC00518 group, and inhibited in the sh-LINC00518 group ($p < 0.05$) (Fig. 2H–I). Then migration of MCF-7 cells was measured by scratch test. The results showed that there was no significant difference in relative migration distance in each group at the 0th h ($p > 0.05$); after 48 h, the relative migration distance in the oe-LINC00518 group increased, the cell migration was increased, the relative migration distance in the sh-LINC00518 group was reduced, and cell migration was inhibited ($p < 0.05$) (Fig. 2J–K). These results suggested that silencing of LINC00518 can promote the apoptosis of BC epithelial cells, inhibit cell growth and proliferation, reduce colony formation ability, and inhibit the ability of invasion and migration.

3.3. LINC00518 down-regulation inactivates the Wnt signaling pathway and inhibits epithelial-mesenchymal transition (EMT) in BC

Subsequently, we adopted TOP/FLASH to determine the effects of LINC00518 on the Wnt signaling pathway. The results showed a significant increase in RLU value of the oe-LINC00518 group and the Wnt signaling pathway was activated; the RLU value in the sh-LINC00518 group decreased significantly, and the Wnt signaling pathway was suppressed ($p < 0.05$) (Fig. 3A). RT-qPCR and Western blot analysis were followed to evaluated the mRNA and protein levels of Wnt signaling pathway-related genes. The results showed that the oe-LINC00518 group promoted the mRNA and protein levels of β-catenin,

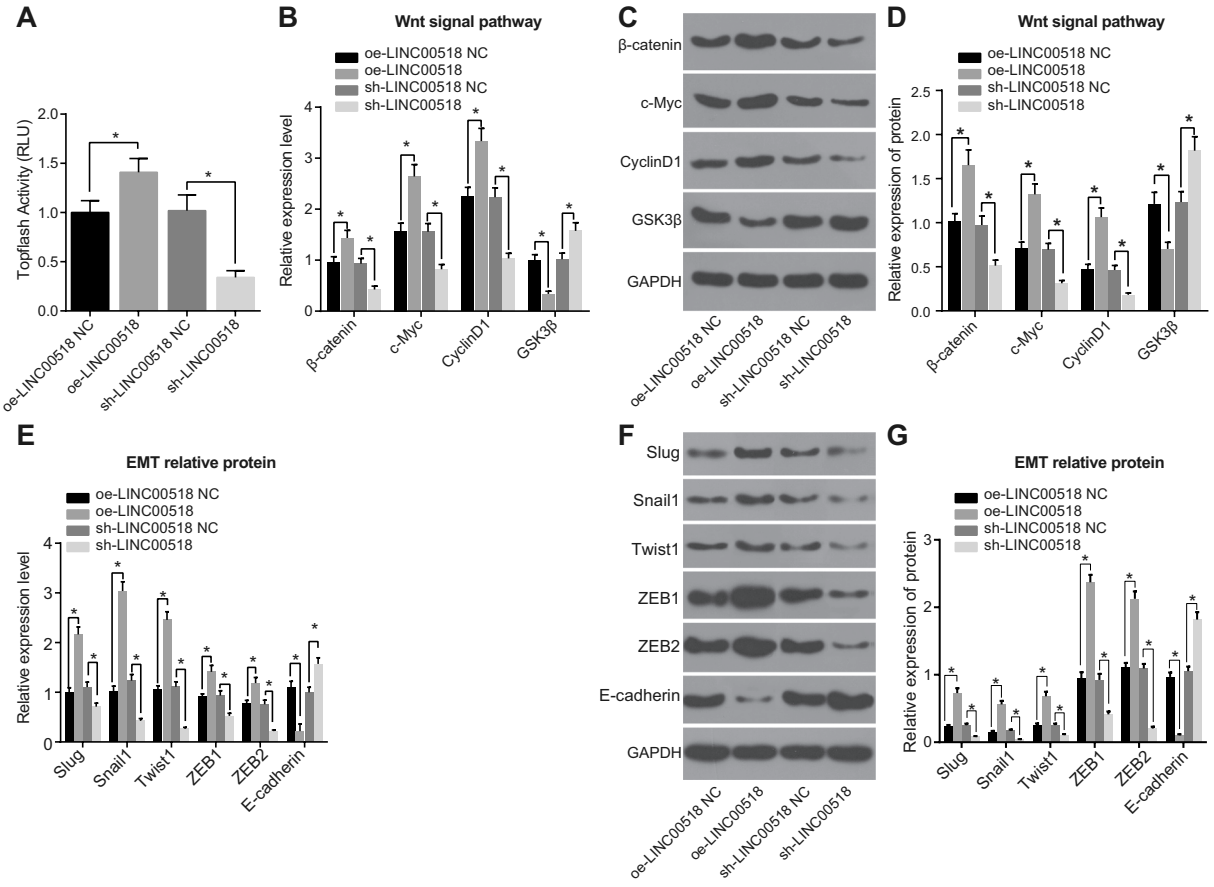

Fig. 3. LINC00518 down-regulation results in the inhibition of the Wnt signaling pathway and hinders EMT in BC. A, quantitative analysis for RLU value of Wnt signaling pathway activation detected by TOP/FLASH; B, quantitative analysis for mRNA levels of β-catenin, c-Myc, CyclinD1 and GSK3β determined by RT-qPCR; C, the gray value of β-catenin, c-Myc, CyclinD1 and GSK3β protein bands measured by Western blot analysis; D, quantitative analysis for protein levels of β-catenin, c-Myc, CyclinD1 and GSK3β; E, quantitative analysis for mRNA levels of Slug, Snail1, Twist1, ZEB1, ZEB2 and E-cadherin tested by RT-qPCR; F, the gray value of Slug, Snail1, Twist1, ZEB1, ZEB2 and E-cadherin protein bands assessed by Western blot analysis; G, quantitative analysis for protein levels of Slug, Snail1, Twist1, ZEB1, ZEB2 and E-cadherin in BC; *, $p < 0.05$ *vs.* the oe-LINC00518 NC and sh-LINC00518 NC groups; the statistical values are measurement data, and the comparison among multiple groups was analyzed by one-way ANOVA; Pairwise comparisons between groups were conducted using least significant difference test; the experiment was repeated 3 times; LINC00518, long intergenic non-coding RNA 518; EMT, epithelial-mesenchymal transition; RT-qPCR, reverse transcription quantitative polymerase chain reaction; RLU, Relative luciferase units; oe, overexpression; NC, negative control.

c-Myc, CyclinD1, inhibited the mRNA and protein levels of GSK3β; and silencing of LINC00518 inhibited the mRNA and protein levels of β-catenin, c-Myc, CyclinD1, and promoted the mRNA and protein levels of GSK3β ($p < 0.05$) (Fig. 3B, C, D). In order to study the relationship between LINC00518 and EMT, RT-qPCR and Western blot analysis were used to measure the mRNA and protein levels of EMT-related factors. The results displayed that oe-LINC00518 group promoted the mRNA and protein levels of Slug, Snail1, Twist1, ZEB1, ZEB2, and inhibited the mRNA and protein levels of E-cadherin; while the sh-LINC00518 group inhibited the mRNA and protein levels of Slug, Snail1, Twist1, ZEB1, ZEB2, and promoted the mRNA and protein levels of E-cadherin ($p < 0.05$) (Fig. 3E, F, G). These results suggested that down-regulation of LINC00518 can prevent Wnt signaling pathway from activation and then inhibit the expression of EMT-related proteins Slug, Snail1, Twist1, ZEB1, ZEB2, and promote the expression of E-cadherin.

3.4. LINC00518 promotes CDX2 methylation

The mRNA levels of CDX2 in BC tissues were determined by RT-qPCR. The results showed that the mRNA levels of CDX2 in BC tissue were significantly lower than that in adjacent normal tissue ($p < 0.05$) (Fig. 4A). The expression of CDX2 in the BC tissue was measured by immunohistochemistry. The results showed that the positive rate of CDX2 protein in BC tissue was significantly lower than that in adjacent normal tissue, and the positive rate of CDX2 protein in the nucleus was brownish yellow ($p < 0.05$) (Fig. 4B–C). The MethPrimer software was used to analyze the CpG island in promoter region of nucleotide sequence with 4200 BP near the CDX2 gene promoter. The results showed that the CpG island existed in the promoter region of CDX2 gene, indicating that the expression of CDX2 gene was affected by promoter methylation (Fig. 4D). In order to prove that the expression of CDX2 gene was affected by promoter methylation, 60 cases of BC and adjacent normal tissues were randomly selected. The methylation level of CpG island in the promoter region of CDX2 gene was assessed by BSP and MSP. The results showed that the methylation level of CDX2 gene promoter region of the BC was higher ($p < 0.05$) and the methylation rate was 76.7% (46/60); while the methylation level of CDX2 gene promoter region of the adjacent normal tissue was lower ($p < 0.05$) and the methylation rate was 18.3% (11/60) (Fig. 4E–F). These results indicated that CDX2 expression was lower in BC, while its methylation level was higher.

The similarity between the promoter region of LINC00518 and CDX2 promoter region was compared with the Blast comparison website to further investigate the correlation between the methylation level of CDX2 gene promoter region and LINC00518. The results showed that there were binding sites of complementary base pairing in the promoter region of LINC00518 and CDX2 (Fig. 4G). The results of dual-luciferase reporter gene assay showed as significant decrease in the luciferase

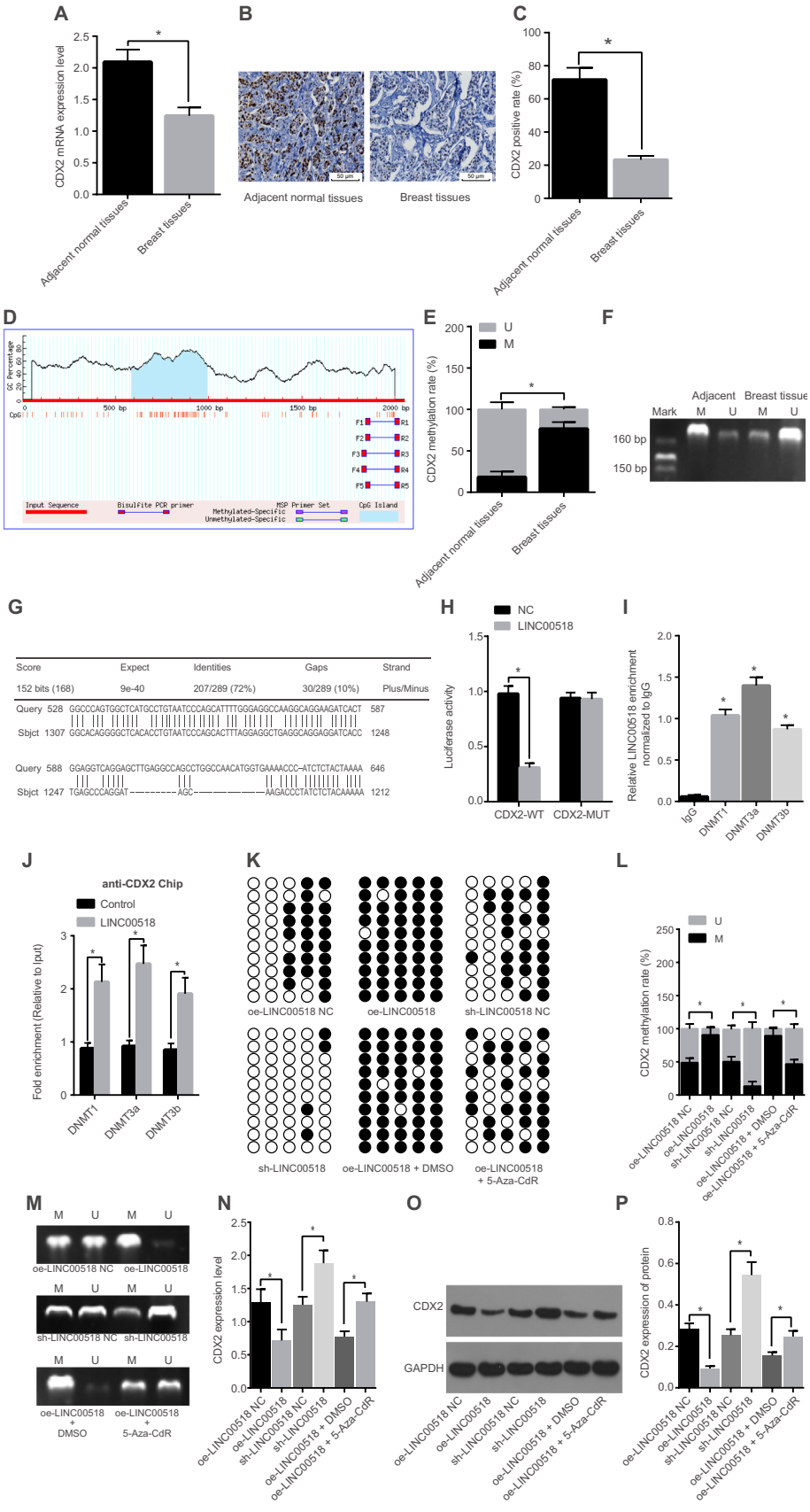

Fig. 4. LINC00518 promotes CDX2 methylation. A, CDX2 mRNA level in BC tissues and adjacent normal tissues determined by RT-qPCR; B, the positive expression of CDX2 in BC tissues and adjacent normal tissues assessed by Immunohistochemistry (200×); C, quantitative analysis for positive expression of CDX2 in BC tissues and adjacent normal tissues; D, distribution of CpG islands in the promoter region of the CDX2 gene; E, quantitative analysis for CDX2 methylation in BC tissues and adjacent normal tissues detected by BSP; F, quantitative analysis for CDX2 methylation level in BC tissues and adjacent normal tissues detected by MSP, which verified the results of BSP; G, Blast comparison found the binding sites of complementary base pairing in the promoter region of LINC00518 and CDX2; H, targeted relationship of LINC00518 to CDX2 confirmed by dual-luciferase report gene assay; I, the enrichment of LINC00518 to methyltransferase (DNMT1 DNMT3a, DNMT3b) in MCF-7 cells detected by RIP; J, the binding of CDX2 promoter to DNA methyltransferase (DNMT1, DNMT3a, DNMT3b) in MCF-7 cells detected by CHIP; K, CDX2 methylation level in MCF-7 cells detected by BSP; L, the quantitative analysis for CDX2 methylation rate in MCF-7 cells detected by BSP; M, CDX2 methylation rate in MCF-7 cells detected by MSP; N, quantitative analysis for CDX2 mRNA levels in MCF-7 cells detected by RT-qPCR; O, gray value of CDX2 protein band in MCF-7 cells detected by Western blot analysis; P, quantitative analysis for CDX2 protein level in MCF-7 cells detected by Western blot analysis; *, $p < 0.05$ *vs.* adjacent normal tissue, or the NC group, or IgG group, or control group, or oe-LINC00518 NC group or sh-LINC00518 NC group or oe-LINC00518 + DMSO group; the statistical data are measurement data; the comparison between two groups was analyzed by *t*-test, comparison among multiple groups by one-way ANOVA and pairwise comparison by the least significant difference; the experiment was repeated 3 times; CDX2, Caudal-related homeobox 2; TCGA, The Cancer Genome Atlas; LINC00518, long intergenic non-coding RNA 518; RT-qPCR, reverse transcription quantitative polymerase chain reaction; CpG, cytosine-phosphate-guanine; BSP, Bisulfite sequencing polymerase chain reaction; MSP, Methylation specific polymerase chain reaction; DNMT, DNA methyltransferase; CHIP, Chromatin immunoprecipitation; RIP, RNA immunoprecipitation; oe, overexpression; NC, negative control; IgG, immunoglobulin G; DMSO, Dimethyl Sulphoxide.

activity of the CDX2-Wt group compared with the NC group ($p < 0.05$), while there were no significant changes observed in luciferase activity of the CDX2-Mut group ($p > 0.05$) (Fig. 4H). It indicated that LINC00518 can bind to the promoter region of CDX2 gene, which was consistent with the prediction result of the bioinformatics website. RIP was used to detect the enrichment of LINC00518 to methyltransferase DNMT1, DNMT3a and DNMT3b. The results showed that there was significant enrichment effect of LINC00518 and methyltransferase in the cell line with high LINC00518 expression (Fig. 4I). Finally, CHIP was used to detect the enrichment of methyltransferase in the promoter region of the CDX2 gene, and it was found that compared with the normal cells, there was also significant enrichment effect of CDX2 promoter region and methyltransferase in the cell line with high LINC00518 expression (Fig. 4J).

The methylation level of CpG island on CDX2 gene promoter in MCF-7 cell line with high expression of LINC00518 and low expression of LINC00518 was detected by BSP and MSP. RT-qPCR and Western blot analysis were used to measure CDX2 expression in MCF-7 cell line with high LINC00518 expression and low expression of LINC00518. The results showed that the CpG island of CDX2 gene showed high methylation in LINC00518 over-expressed cells (Fig. 4K, L, M), and the expression of CDX2 decreased (Fig. 4N, O, P); in LINC00518 low-expressed cells, the methylation level also decreased (Fig. 4K, L, M), and the expression of CDX2 increased (Fig. 4N, O, P). The DNA methyltransferase inhibitor 5-Aza-CdR was used to demethylate the promoter region of CDX2 gene in order to further explore the regulatory mechanism between LINC00518 and CDX2 gene. The results of BSP and MSP showed that the methylation level of CDX2 in the oe-LINC00518 + DMSO group in MCF-7 cell line increased significantly (Fig. 4K, L, M), and CDX2 expression decreased (Fig. 4N, O, P). With the addition of 5-Aza-CdR, the methylation level of CDX2 in MCF-7 cell line was significantly decreased (Fig. 4K, L, M), and CDX2 expression increased (Fig. 4N, O, P). These findings indicated that there was a significant correlation between the methylation level of CpG island in the promoter region of the CDX2 gene and the expression of LINC00518, and the effect of LINC00518 on methylation of CDX2 promoter region was mediated by the methyltransferase.

3.5. CDX2 overexpression promotes BC epithelial cell apoptosis, and inhibits cell growth and proliferation, invasion and migration

In order to study the effect of CDX2 on the proliferation, apoptosis, invasion and migration of MCF-7 cells, MCF-7 cells were transfected with CDX2 high-expression plasmid to interfere the expression of CDX2 in MCF-7 cells. Then CCK-8 was used to test the proliferation of MCF-7 cells in each group. The results showed that under the same initial concentration, the OD values at the 24th h were not different ($p > 0.05$), and the overexpression of CDX2 significantly decreased the OD values of MCF-7 cells at the 48th h, 72nd h, 96th h, and MCF-7 cell proliferation was inhibited ($p < 0.05$) (Fig. 5A). Edu method was used to re-verify the proliferation of MCF-7 cells in each group. The results revealed that the red positive cells in the oe-CDX2 group were significantly reduced ($p < 0.05$) (Fig. 5B–C). Colony formation assay was used to determine colony formation ability of MCF-7 cells after transfection. Results displayed that the oe-CDX2 group inhibited colony formation ($p < 0.05$) (Fig. 5D–E). The apoptosis of MCF-7 cells was examined by TUNEL, and the results showed that the apoptotic cells were stained with green fluorescence, and the oe-CDX2 group promoted the apoptosis of MCF-7 cells ($p < 0.05$) (Fig. 5F–G). The invasion of MCF-7 cells was tested by Transwell assay. The results revealed that overexpression of CDX2 inhibited cell invasion ($p < 0.05$) (Fig. 5H–I). The migration of MCF-7 cells was evaluated by scratch test. The results showed that there was no significant difference in relative migration distance between each group at the 0th h ($p > 0.05$); after 48 h, the relative migration distance of the oe-CDX2 group was reduced, and cell migration was inhibited ($p < 0.05$) (Fig. 5J–K). The above results indicated that overexpression of CDX2 can promote the apoptosis of BC epithelial cells, inhibit cell growth and proliferation, reduce colony formation ability, and inhibit the ability of invasion and migration.

3.6. CDX2 overexpression blocks the Wnt signaling pathway and inhibits EMT in BC

TOP/FLASH was applied to detect the activation of Wnt signaling pathway for the purpose of evaluating the relationship between CDX2 and the Wnt signaling pathway. The results showed that the RLU value of the oe-CDX2 group was significantly decreased, the Wnt signaling pathway was inhibited ($p < 0.05$) (Fig. 6A). RT-qPCR and Western blot analysis were used to measure the mRNA and protein levels of CDX2 and the Wnt signaling pathway-related factors. The results demonstrated that overexpression of CDX2 inhibited the mRNA and protein levels of β-catenin, c-Myc, CyclinD1, promoted the mRNA and protein levels of CDX2 and GSK3β ($p < 0.05$) (Fig. 6B, C, D). In order to study the relationship between CDX2 and EMT, RT-qPCR and Western blot analysis were used to determine the mRNA and protein levels of EMT-related factors. The results displayed that overexpression of CDX2 could inhibit the mRNA and protein levels of Slug, Snail1, Twist1, ZEB1, ZEB2, and promote the mRNA and protein levels of E-cadherin ($p < 0.05$) (Fig. 6E, F, G). The above results suggested that overexpression of CDX2 can inhibit the activation of Wnt signaling pathway and then repress the expression of EMT-related proteins Slug, Snail1, Twist1, ZEB1, ZEB2, yet promote the expression of E-cadherin.

3.7. LINC00518 down-regulation inhibits growth and metastasis of BC

In order to further analyze the effect of LINC00518 expression on the growth and metastasis of BC *in vivo*, the MCE-7 cells transfected with oe-LINC00518 and sh-LINC00518 were inoculated into nude mice. The growth and weight analysis of tumor volume in nude mice showed that the tumor growth of nude mice inoculated with MCF-7 cells transfected with oe-LINC00518 was significantly faster than that of the control group (Fig. 7A, B), the weight increased (Fig. 7C), and the volume increased (Fig. 7D) ($p < 0.05$). The growth rate of MCF-7 cells transfected with sh-LINC00518 was slower than that of the control group (Fig. 7A, B), the weight decreased (Fig. 7C), and the volume was smaller (Fig. 7D) (all $p < 0.05$). In order to study the lymph node metastasis, the paraffin specimens were made from axillary lymph nodes after nude mice were euthanized at the 28th day. The lymph node metastasis was observed using HE staining, the results of which showed that the cancer cells of axillary lymph nodes in the nude mice were irregular in shape, split, with large nucleus, deep staining and large nucleoplasm, and low differentiation. Compared with the control group, 7 of 8 nude mice in the oe-LINC00518 group were positive for lymph node metastasis, and the positive rate of metastasis was 87.5%. The number of tumor cells in the HE section was obviously higher than that in the other groups. Compared with the control group, 2 of 8 nude mice in the sh-LINC00518 group were positive for lymph node metastasis, and the positive rate of metastasis was 25%. The number of tumor cells in the HE section was obviously lower than that of the other groups ($p < 0.05$) (Fig. 7E, F). It was demonstrated that LINC00518 overexpression can lead to the proliferation and metastasis of BC, while silencing of LINC00518 can result in inhibited growth and metastasis of BC.

In order to further analyze whether the interaction of LINC00518 and CDX2 affects the growth and metastasis of BC, the MCE-7 cells transfected with oe-LINC00518 + oe-CDX2 were inoculated in nude mice, and oe-LINC00518 + oe-CDX2 NC was set as control. The results revealed a significant decrease in tumor growth, volume and tumor weight in the oe-LINC00518 + oe-CDX2 group (Fig. 7A–D), and 3 of the 8 nude mice were positive for lymph node metastasis, and the positive rate of metastasis was 37.5%. The number of tumor cells in HE slices was obviously lower than that of the oe-LINC00518 + oe-CDX2 NC

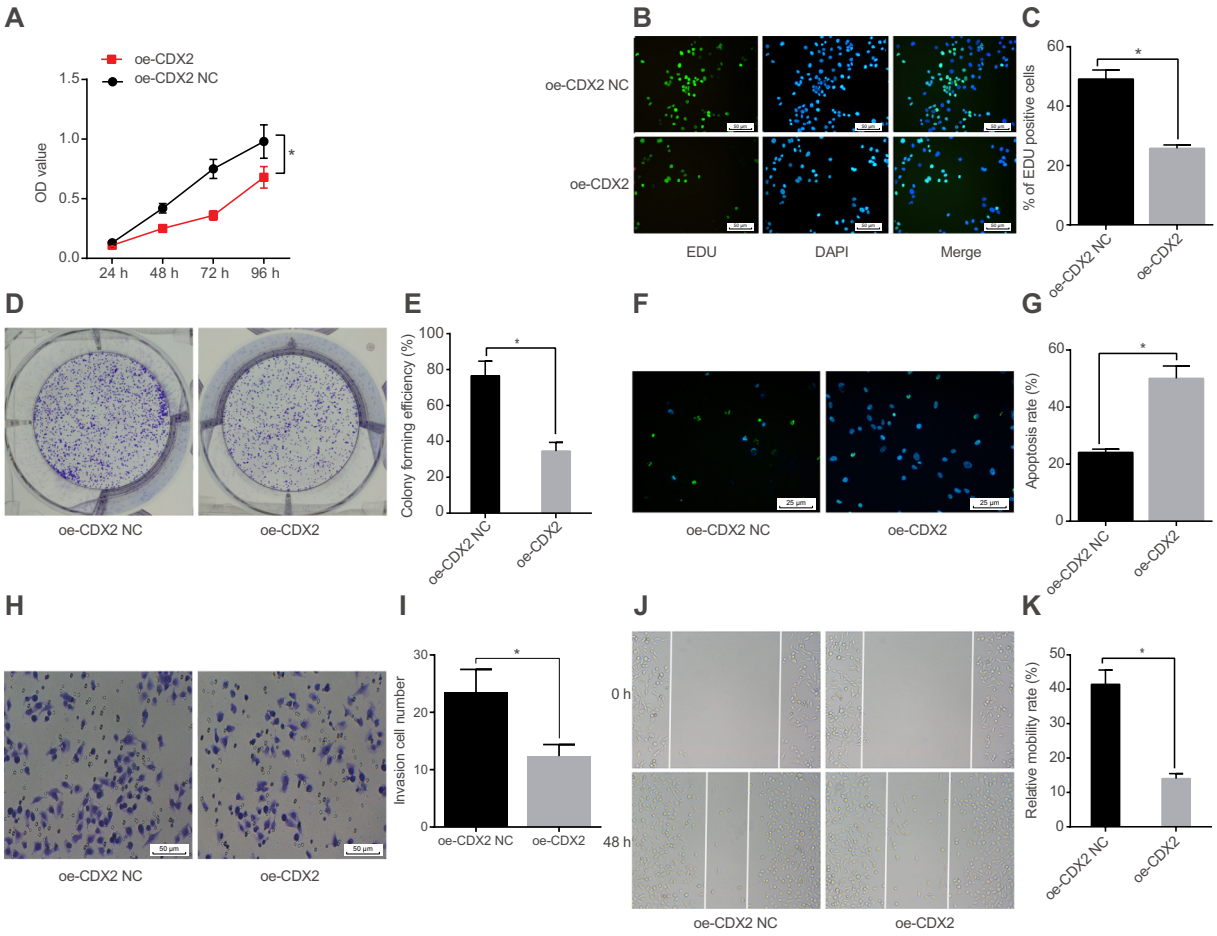

Fig. 5. The overexpression of CDX2 leads to the acceleration of BC epithelial cell apoptosis, inhibits cell growth and proliferation, invasion and migration. A, OD value of BC epithelial cells detected by CCK-8 and analyzed by two-way ANOVA; B, BC epithelial cell proliferation and fluorescence staining (200×) detected by Edu assay; C, quantitative analysis for BC epithelial cell proliferation level; D, colony formation of BC epithelial cells measured by dual soft-agar colony formation assay; E, quantitative analysis for BC epithelial cell colony formation level; F, apoptosis of BC epithelial cells detected by TUNEL staining (400×); G, quantitative analysis for apoptosis rate of BC epithelial cells; H, invasion ability of BC epithelial cells detected by Transwell assay (200×); I, quantitative analysis for BC epithelial cell invasion rate; J, the migration distance of BC epithelial cells detected by scratch test (100×); K, quantitative analysis for BC epithelial cell migration rate, and the data were analyzed by *t*-test; *, $p < 0.05$ *vs.* the oe-CDX2 NC group; the data are measurement data, and experiment was repeated 3 times; BC, breast cancer; CDX2, Caudal-related homeobox 2; OD, optical value; CCK-8, Cell Counting Kit-8; Edu, 5-ethynyl-2′-deoxyuridine; TUNEL, Terminal deoxynucleotidyl transferase (TdT)-mediated dUTP nick end labeling; oe, overexpression; NC, negative control.

group (Fig. 7E, F) ($p < 0.05$). It was indicated that downregulation of LINC00518 elevated CDX2 expression and then reversed the rapid growth and metastasis process induced by LINC00518 overexpression.

3.8. LINC00518 down-regulation represses the Wnt signaling pathway activation and EMT process in vivo by reducing CDX2 methylation

The positive expression of CDX2 in BC tissues of nude mice was measured by immunohistochemistry. The results showed that CDX2 was located in the nucleus and the positive expression was brownish yellow. Compared with the sh-LINC00518 NC group, the sh-LINC00518 group promoted the positive expression of CDX2 ($p < 0.05$) (Fig. 8A, B). The mRNA level of CDX2 in nude mice was determined by RT-qPCR. The results showed that compared with the sh-LINC00518 NC group, the sh-LINC00518 group promoted CDX2 mRNA levels ($p < 0.05$) (Fig. 8C). The activation of Wnt signaling pathway was detected by TOP/FLASH, and based on the results, the RLU value of the sh-LINC00518 group was significantly lower than that of the sh-LINC00518 NC group, and the Wnt signaling pathway was suppressed ($p < 0.05$) (Fig. 8D). Western blot analysis was used to examine the expression of Wnt signaling pathway-related proteins, finding that compared with the sh-LINC00518 NC group, the sh-LINC00518 group inhibited protein levels of β-catenin, c-Myc and CyclinD1, and promoted GSK3β level ($p < 0.05$) (Fig. 8E and F). Western blot analysis was further used to test the protein levels of EMT-related proteins, revealing that compared with the sh-LINC00518 NC group, the sh-LINC00518 group inhibited protein levels of Slug, Snail1, Twist1, ZEB1 and ZEB2, and promoted the E-cadherin level ($p < 0.05$) (Fig. 8G and H). It was indicated that LINC00518 can promote CDX2 methylation *in vivo*, inhibit CDX2 expression, activate Wnt signaling pathway, and promote EMT.

The effects of LINC00518 expression on CDX2, Wnt signaling pathway and EMT were subsequently explored. The results showed that, compared with the oe-LINC00518 + oe-CDX2 NC group, the positive expression rate of CDX2 in the oe-LINC00518 + oe-CDX2 group was significantly higher ($p < 0.05$) (Fig. 8A, B), the mRNA levels of CDX2 were significantly increased ($p < 0.05$) (Fig. 8C), the RLU value decreased significantly, and the Wnt signal pathway was suppressed (Fig. 8D). The expression of β-catenin, c-Myc, CyclinD1, Slug, Snail1, Twist1, ZEB1 and ZEB2 was inhibited ($p < 0.05$), and the expression of GSK3β and E-cadherin was induced ($p < 0.05$) (Fig. 8E, F, G, H). These results suggested that LINC00518 promoted CDX2 methylation, inhibited the expression of CDX2, activated the Wnt signaling pathway and promoted EMT. After the up-regulation of CDX2 expression, the

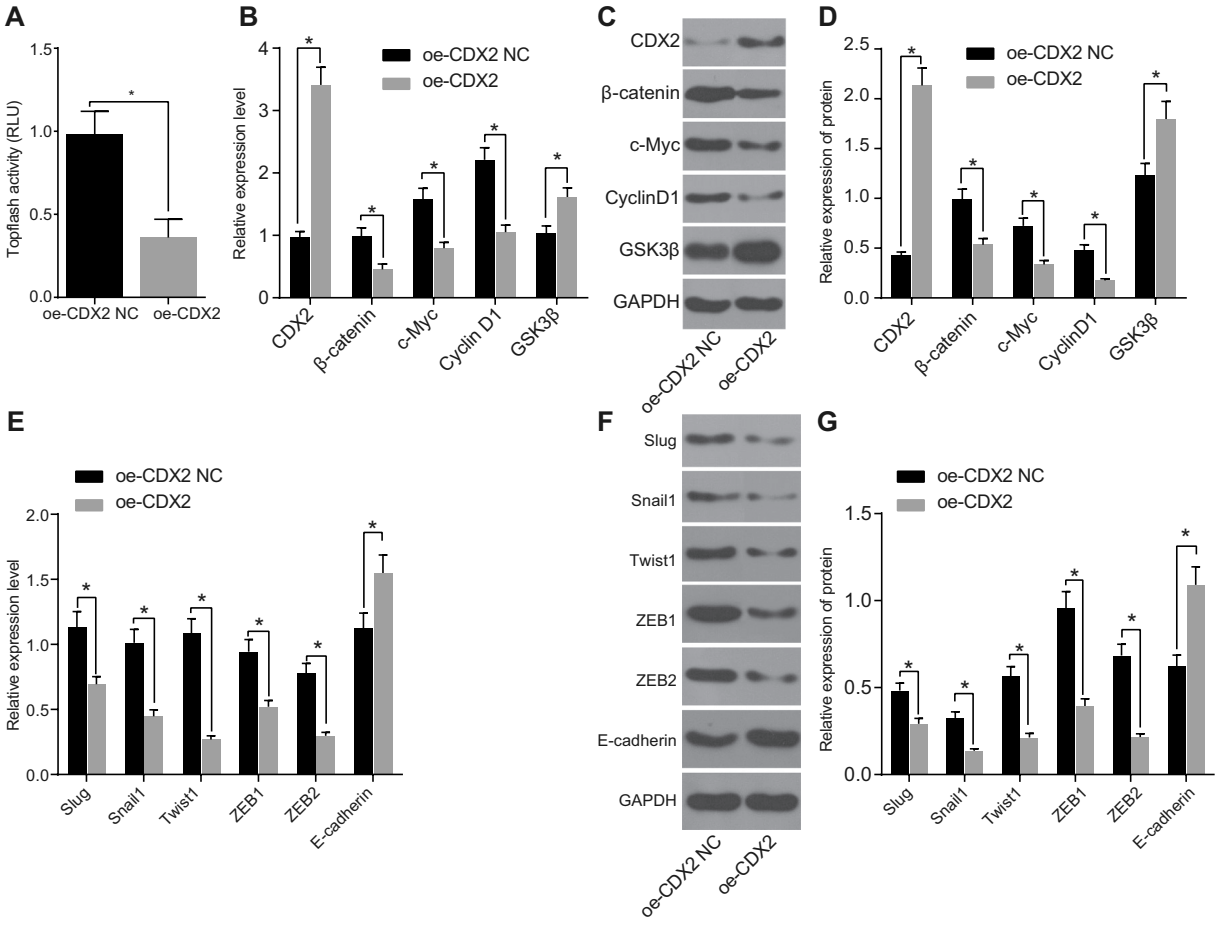

Fig. 6. Overexpressed CDX2 inhibits the activation of Wnt signaling pathway and suppresses the expression of EMT-related proteins Slug, Snail1, Twist1, ZEB1, ZEB2, yet promotes the expression of E-cadherin. A, quantitative analysis for RLU value and Wnt signaling pathway activation detected by TOP/FLASH; B, quantitative analysis for mRNA levels of Wnt signaling pathway-related genes detected by RT-qPCR; C, protein bands of Wnt signaling pathway-related genes detected by Western blot analysis; D, quantitative analysis for protein levels of Wnt signaling pathway related factor detected by Western blot analysis; E, quantitative analysis for the mRNA levels of EMT-related genes detected by RT-qPCR; F, protein bands of EMT-related genes detected by Western blot analysis; G, protein level quantitative analysis for EMT related factor detected by Western blot analysis; *, $p < 0.05$ *vs.* the oe-CDX2 NC group; the statistical values are measurement data, and pairwise comparison was analyzed by *t*-test; the experiment was repeated 3 times; CDX2, Caudal-related homeobox 2; EMT, epithelial-mesenchymal transition; RT-qPCR, reverse transcription quantitative polymerase chain reaction; TOP/FLASH, T cell factor Optimal Promoter + luciferase; RLU, Relative luciferase units; oe, overexpression; NC, negative control.

promoting effects of LINC00518 on Wnt signaling pathway and promoted EMT was reversed.

4. Discussion

BC remains to be a major cause of morbidity and mortality among the female population, which is mainly due to the high potential of regional and/or distal metastasis of the primary breast tumors [31]. Based on previously reported studies, lincRNAs might play a key role in the development and progression of BC [32,33]. Our study explored the effect of LINC00518 on the growth and metastasis of BC epithelial cells *via* the Wnt signaling pathway by binding to CDX2 gene. The results showed that the down-regulation of LINC00518 expression resulted in the enhancement of CDX2 expression through the inhibition of CDX2 methylation and Wnt signaling pathway activation, which in turn leads to the suppression of proliferation, invasion and metastasis of BC epithelial cells while it promotes apoptosis (Fig. 9).

Initially, data obtained in the present study demonstrated that there was a high expression in LINC00518 in BC tissues and cells. LncRNAs exert important functions in the occurrence and development of tumor. An example would be the enhancement of EMT and the formation of new blood vessels in BC epithelial cells as a result of HOTAIR up-regulation [34]. Based on the co-expression networks provided by Yang et al., lncRNAs was identified as a potential core in the triple-negative BC, where LINC00518 is the most up-regulated [35]. LINC00518 expression is observed as a sensitive and effective target when detecting cutaneous melanoma [36]. The present study also demonstrated that silencing of LINC00518 or overexpression of CDX2 can promote the apoptosis of BC epithelial cells, inhibit cell growth and proliferation, invasion and migration and reduce colony formation ability. A research conducted by Jonsson et al. suggested that silencing of lincRNA LINC00160 reduced proliferation and promoted survival of MCF7 BC cells. [37].

Moreover, our results displayed that LINC00518 promoted CDX2 methylation through the methyltransferase and reduced CDX2 expression. It has been reported that regulation of CDX2 expression by promoter methylation could control the intestinal metaplasia of the esophagus in esophageal adenocarcinoma [38]. It has been observed that the cell proliferation can be enhanced in gastric cancer as a result of the silencing CDX2 expression *via* DNA methylation by microRNA-9 through the binding site in the 3′-UTR [39]. In the present study, there was a low expression in CDX2 in BC and an increased methylation level of CDX2 gene promoter region. Elevated CDX2 methylation in the promoter region was reported to be associated with decreased mRNA

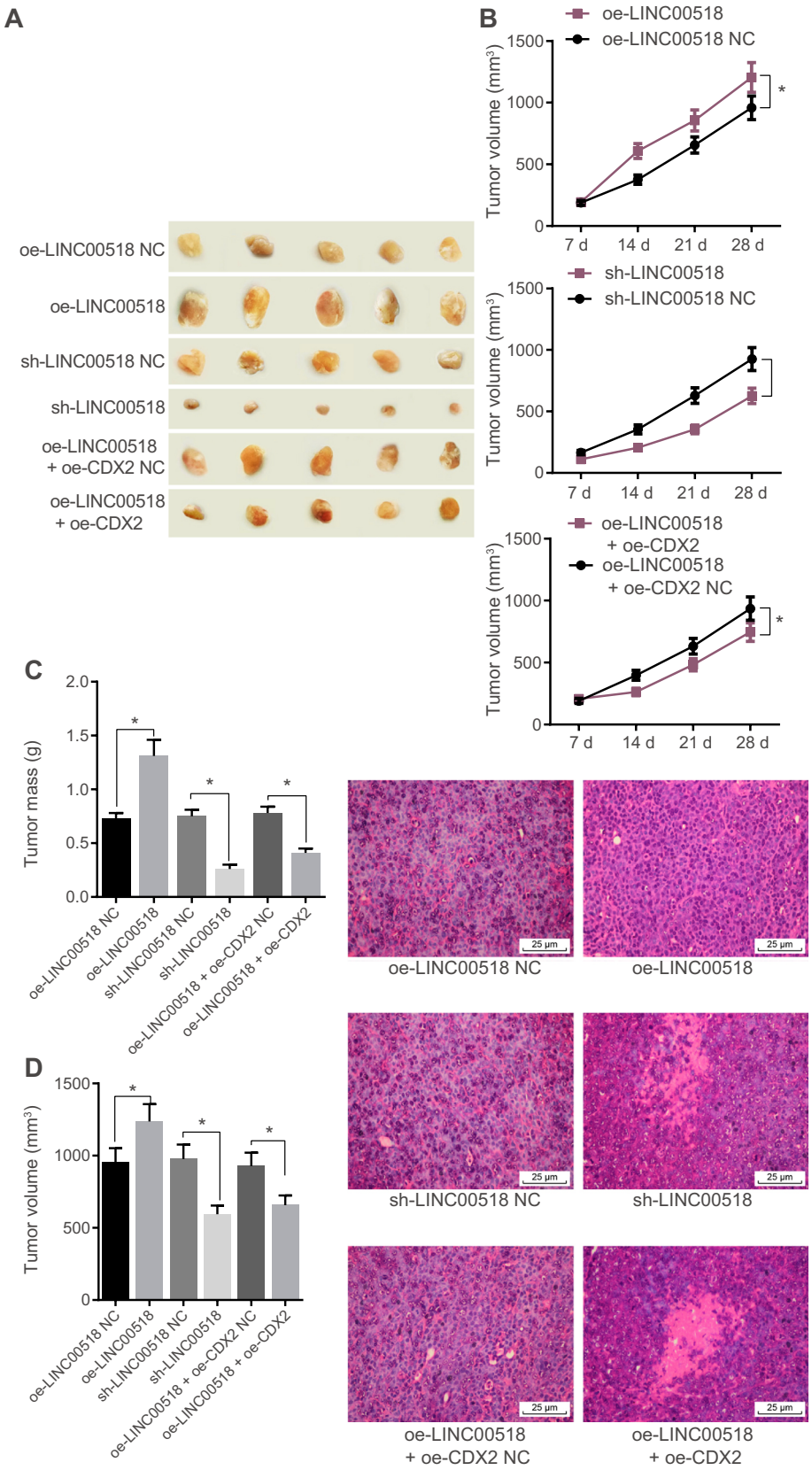

Fig. 7. LINC00518 down-regulation inhibits the growth and metastasis of BC by increasing CDX2 expression. A, tumor sizes of nude mice transfected with oe-LINC00518, sh-LINC00518 or oe-LINC00518 + oe-CDX2; B, tumor volume of nude mice transfected with oe-LINC00518, sh-LINC00518 or oe-LINC00518 + oe-CDX2; C, quantitative analysis for tumor weight indicates that sh-LINC00518 reduces tumor weight; D, quantitative analysis for tumor volume at the 28th day indicates that sh-LINC00518 reduces tumor volume; E, lymph node metastases in nude mice observed following HE staining (400×); F, quantitative analysis for positive rate of lymph node metastasis; *, $p < 0.05$ *vs.* the oe-LINC00518 NC group, or sh-LINC00518 NC group or oe-LINC00518 + oe-CDX2 NC group; the statistical values are measurement data; the comparison at different time points were analyzed by repeated-measures analysis of variance, comparison among multiple groups by one-way ANOVA and pairwise comparison by the least significant difference; the experiment was repeated 3 times; BC, breast cancer; CDX2, Caudal-related homeobox 2; EMT, epithelial-mesenchymal transition; LINC00518, long intergenic non-coding RNA 518; HE, Hematoxylin and eosin; oe, overexpression; NC, negative control.

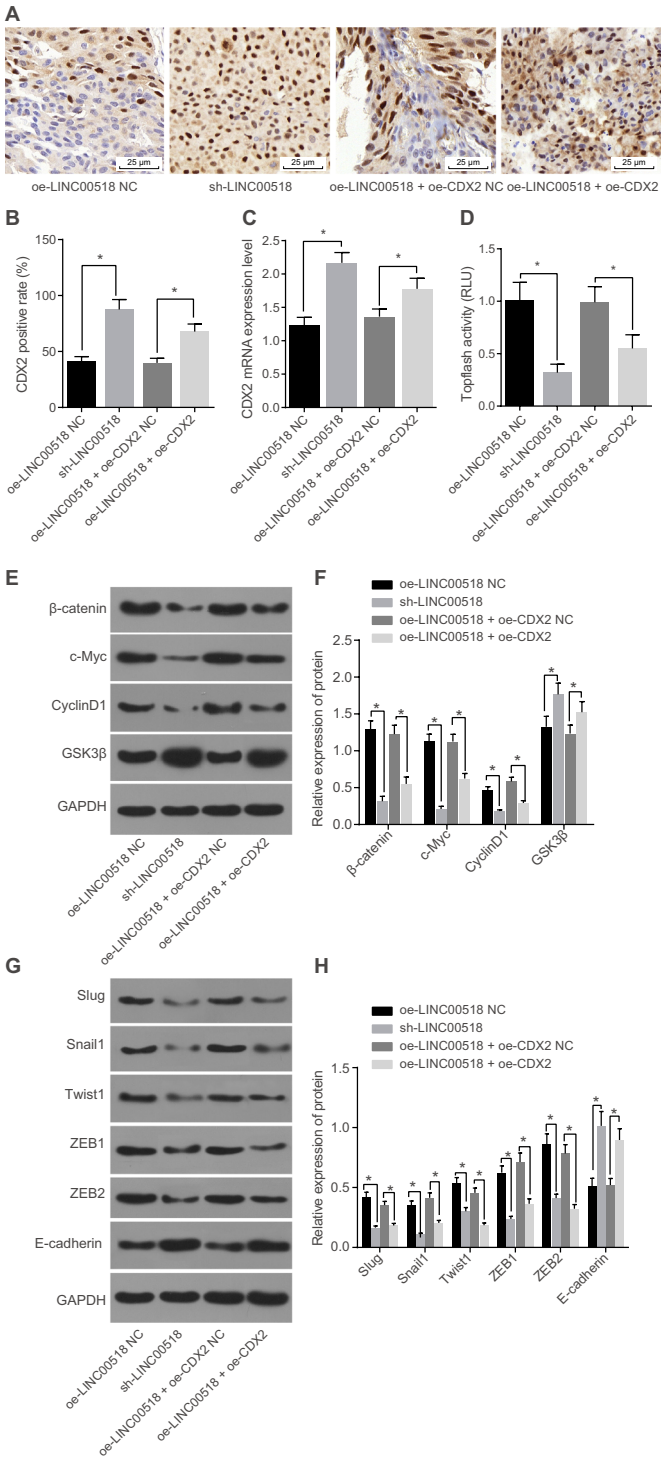

Fig. 8. LINC00518 down-regulation blocks Wnt signaling pathway and reduces EMT *in vivo* by inhibiting CDX2 methylation. A, the positive expression of CDX2 in tumor tissues of each group detected by Immunohistochemical staining (400×; B, quantitative analysis for positive expression of CDX2 in tumor tissues indicates that sh-LINC00518 promoted the positive expression of CDX2; C, quantitative analysis for CDX2 mRNA levels in nude mice tumor tissues detected by RT-qPCR; D, quantitative analysis for RLU value and Wnt signaling pathway activation detected by TOP/FLASH; E, the gray value of β-catenin, c-Myc, CyclinD1 and GSK3β protein bands detected by Western blot analysis; F, quantitative analysis for protein levels of β-catenin, c-Myc, CyclinD1 and GSK3β detected by Western blot analysis; G, the gray value of Slug, Snail1, Twist1, ZEB1, ZEB2 and *E*-cadherin protein bands detected by Western blot analysis; H, quantitative analysis for protein levels of Slug, Snail1, Twist1, ZEB1, ZEB2 and E-cadherin detected by Western blot analysis; *, $p < 0.05$ *vs.* the sh-LINC00518 NC group or oe-LINC00518 + oe-CDX2 NC; the statistical values are measurement data, and the comparison among multiple groups was analyzed by one-way ANOVA and pairwise comparison by the least significant difference; the experiment was repeated 3 times; RT-qPCR, reverse transcription quantitative polymerase chain reaction; CDX2, Caudal-related homeobox 2; LINC00518, long intergenic non-protein coding RNA 518; EMT, epithelial-mesenchymal transition; TOP/FLASH, T cell factor Optimal Promoter + luciferase; RLU, Relative luciferase units; oe, overexpression; NC, negative control.

levels, gene silencing in colorectal cancer patients with lymph node metastasis and shorter survival time [40]. A recent study found that methylation of the promoter region of CDX2 gene resulted in an increase in the incidence rate of colorectal cancer [41]. In addition, overexpression of CDX2 was also shown to inhibit the growth and migration of xenograft colorectal tumors in nude mice [42].

Our results also found that the silencing of LINC00518 and over-expression of CDX2 leads to suppressed expression of β-catenin, c-Myc, and CyclinD1, while promoted GSK3β expression, and inhibited activation of Wnt signaling pathway. β-catenin, c-Myc, and CyclinD1 are key participants in the Wnt signaling pathway, in which aberrancies have been associated with malignant cell transformation [43]. GSK3β acts as a key inhibitor of the Wnt-β-catenin signaling pathway [44]. S100A7-overexpressing estrogen receptor α-positive in BC cells induced the down-regulation of β-catenin, CyclinD1, and c-Myc and up-regulation of GSK3β [45]. In addition, adenomatosis polyposis down-regulated 1 (APCDD1), a membrane-boundglyco protein, inhibits the Wnt signaling pathway by binding to WNT3A and LRP5 [46]. Recently, it has been found that the human calcium-channel β_4-subunit gene (CACNB4) inhibits the Wnt signaling pathway through the inhibition of TCF4 activity [47]. Furthermore, the Wnt signaling pathway can be suppressed by the hedgehog pathway through sFRP-1 [48]. Based on the above findings, it could be concluded that the inhibitory components of the Wnt signaling pathway are complex. CDX2 was screened out as the target gene of LINC00518 in order to further investigate the downstream target gene of LINC00518 which blocks the Wnt signaling pathway. Similarly, CDX2 serves as a Wnt signaling inhibitor and is frequently silenced by promoter hypermethylation in lung cancer as a tumor suppressor [49]. Tóth et al. further documented that silencing of CDX2 gene is linked with DNA repair proteins and is a key factor of the Wnt signaling pathway in colorectal cancer with liver metastasis [50]. Furthermore, our study presented that silencing of LINC00518 and overexpression of CDX2 lead to the suppression of the EMT-related proteins Slug, Snail1, Twist1, ZEB1, ZEB2, and promoted expression of *E*-cadherin. Transcription factors, Snail1, Twist1, ZEB1, and ZEB2, as well as loss of E-cadherin have been reported to induce EMT, thus facilitating tumor metastasis [51,52]. The silencing of LINC00518 expression and over-expression of CDX2 results in the inhibition of EMT, which then leads to the inhibition of proliferation, invasion and migration of BC epithelial cells.

In conclusion, the key findings of the study demonstrated that down-regulated LINC00518 promoted CDX2 expression through the suppression of CDX2 methylation and inhibition of Wnt signaling pathway activation, whereby inhibiting proliferation, invasion and EMT of BC epithelial cells, as well as lymph node metastasis. This study may provide a potential therapeutic target for the treatment of BC in the future. However, due to the limitation we faced in experimental conditions and funds, we weren't able to provide other possible target genes in this study. Therefore, further studies are required to further illustrate the mechanisms involved in BC.

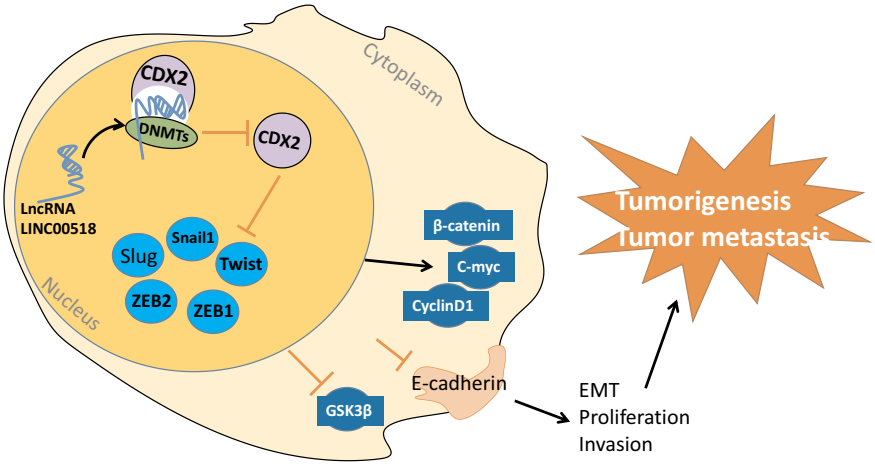

Fig. 9. The mechanistic map illustrating effects of LINC00518 on the growth and metastasis of breast cancer cells. LINC00518 expression increases the DNMT of CDX2 and thus inhibiting the expression of CDX2 gene, under which condition, the Wnt signaling pathway was activated. Resultantly, the BC cell proliferation, EMT and invasion were promoted, thereby the metastasis of BC was promoted. DNMT, DNA methyltransferase; EMT, epithelial-mesenchymal transition.

Abbreviations

BC	Breast cancer
EMT	epithelial-mesenchymal transition
lincRNAs	Long intergenic noncoding RNAs
LINC00518	Long intergenic non-protein coding RNA 518
CDX2	Caudal-related homeobox 2
WHO	World Health Organization
AJCC	American Joint Committee on Cancer
TNM	Tumor-Node-Metastasis
IgG	immunoglobulin G
HRP	horseradish peroxidase
DAB	diaminobenzidine
BSP	Bisulfite sequencing polymerase
MSP	Methylation specific polymerase
RT-qPCR	Reverse transcription quantitative polymerase chain reaction
BCA	bicinchoninic acid
PAGE	polyacrylamide gel electrophoresis
PVDF	polyvinylidene fluoride
BSA	bovine serum albumin
GSK3β	Glycogen synthase kinase 3beta
ZEB	Zinc finger E-box
GAPDH	glyceraldehyde-3-phosphate dehydrogenase
DMEM	Dulbecco's modified Eagle's medium
FBS	fetal bovine serum
DMSO	dimethyl sulphoxide
TOPflash	T cell factor optimal promoter
RLU value	Relative luciferase units
FISH	Fluorescence *in situ* hybridization
DAPI	diamidino-2-phenylindole
PBS	phosphate buffer saline
RIP	RNA immunoprecipitation
DNMT	DNA methyltransferase
CHIP	Chromatin immunoprecipitation
CCK-8	Cell counting kit-8
EDU	ethynyl-2′-deoxyuridine
TdT	Terminal deoxynucleotidyl transferase
TUNEL	transferase-mediated dUTP nick end labeling
POD	peroxidase
AI	apoptotic index
SPF	specific pathogen-free
LSD	least significant difference
OD	optical density

Conflict of interest

The authors declare that they have no competing interests.

Transparency document

The Transparency document associated with this article can be found, in online version.

Acknowledgments

We would like to acknowledge the reviewers for their helpful comments on this paper.

Funding

This study was supported by Harbin Applied Technology Research and Development Project Plan (Harbin Science and Technology Bureau) (No. 2016RAQXJ174).

Availability of data and materials

The datasets generated/analyzed during the current study are available.

Authors' contributions

HBW and HW designed the study. JSW and LL collated the data, designed and developed the database, carried out data analyses and produced the initial draft of the manuscript. AYC and ZGL contributed to drafting the manuscript. All authors have read and approved the final submitted manuscript.

Ethics approval and consent to participate

The study was conducted following with the approval of the Ethics Committee of Harbin Medical University Cancer Hospital. All participating patients signed informed consent documentation. All animal procedures were conducted in accordance with the National Institutes of Health Guide for the Care and Use of Laboratory Animals (National Institutes of Health, Bethesda, MA, USA). The animals received humane care based on the guideline of Guidebook for the Care and Use of Laboratory Animals.

Consent for publication

Not applicable.

References

[1] B. Sathian, S.B. Nagaraja, I. Banerjee, J. Sreedharan, A. De, B. Roy, E. Rajesh, S. Senthilkumaran, S.A. Hussain, R.G. Menezes, Awareness of breast cancer warning

signs and screening methods among female residents of Pokhara valley, Nepal, Asian Pac. J. Cancer Prev. 15 (2014) 4723–4726.
[2] S. Banerji, K. Cibulskis, C. Rangel-Escareno, K.K. Brown, S.L. Carter, A.M. Frederick, M.S. Lawrence, A.Y. Sivachenko, C. Sougnez, L. Zou, M.L. Cortes, J.C. Fernandez-Lopez, S. Peng, K.G. Ardlie, D. Auclair, V. Bautista-Pina, F. Duke, J. Francis, J. Jung, A. Maffuz-Aziz, R.C. Onofrio, M. Parkin, N.H. Pho, V. Quintanar-Jurado, A.H. Ramos, R. Rebollar-Vega, S. Rodriguez-Cuevas, S.L. Romero-Cordoba, S.E. Schumacher, N. Stransky, K.M. Thompson, L. Uribe-Figueroa, J. Baselga, R. Beroukhim, K. Polyak, D.C. Sgroi, A.L. Richardson, G. Jimenez-Sanchez, E.S. Lander, S.B. Gabriel, L.A. Garraway, T.R. Golub, J. Melendez-Zajgla, A. Toker, G. Getz, A. Hidalgo-Miranda, M. Meyerson, Sequence analysis of mutations and translocations across breast cancer subtypes, Nature 486 (2012) 405–409.
[3] L.A. Torre, F. Bray, R.L. Siegel, J. Ferlay, J. Lortet-Tieulent, A. Jemal, Global cancer statistics, 2012, CA Cancer J. Clin. 65 (2015) 87–108.
[4] M. Riaz, B. Setyono-Han, M.A. Timmermans, A.M. Trapman, J. Bolt-de Vries, A. Hollestelle, R.C. Janssens, M.P. Look, M. Schutte, J.A. Foekens, J.W. Martens, Growth and metastatic behavior of molecularly well-characterized human breast cancer cell lines in mice, Breast Cancer Res. Treat. 148 (2014) 19–31.
[5] Z. Zhang, J. Wang, K.A. Skinner, M. Shayne, S.I. Hajdu, H. Bu, D.G. Hicks, P. Tang, Pathological features and clinical outcomes of breast cancer according to levels of oestrogen receptor expression, Histopathology 65 (2014) 508–516.
[6] M. Apostolopoulou, L. Ligon, Cadherin-23 mediates heterotypic cell-cell adhesion between breast cancer epithelial cells and fibroblasts, PLoS One 7 (2012) e33289.
[7] S.D. McAllister, R. Murase, R.T. Christian, D. Lau, A.J. Zielinski, J. Allison, C. Almanza, A. Pakdel, J. Lee, C. Limbad, Y. Liu, R.J. Debs, D.H. Moore, P.Y. Desprez, Pathways mediating the effects of cannabidiol on the reduction of breast cancer cell proliferation, invasion, and metastasis, Breast Cancer Res. Treat. 129 (2011) 37–47.
[8] M. Mackiewicz, K. Huppi, J.J. Pitt, T.H. Dorsey, S. Ambs, N.J. Caplen, Identification of the receptor tyrosine kinase AXL in breast cancer as a target for the human miR-34a microRNA, Breast Cancer Res. Treat. 130 (2011) 663–679.
[9] X. Ding, L. Zhu, T. Ji, X. Zhang, F. Wang, S. Gan, M. Zhao, H. Yang, Long intergenic non-coding RNAs (LincRNAs) identified by RNA-seq in breast cancer, PLoS One 9 (2014) e103270.
[10] P. Hou, Y. Zhao, Z. Li, R. Yao, M. Ma, Y. Gao, L. Zhao, Y. Zhang, B. Huang, J. Lu, LincRNA-ROR induces epithelial-to-mesenchymal transition and contributes to breast cancer tumorigenesis and metastasis, Cell Death Dis. 5 (2014) e1287.
[11] H. Zhang, K. Cai, J. Wang, X. Wang, K. Cheng, F. Shi, L. Jiang, Y. Zhang, J. Dou, MiR-7, inhibited indirectly by lincRNA HOTAIR, directly inhibits SETDB1 and reverses the EMT of breast cancer stem cells by downregulating the STAT3 pathway, Stem Cells 32 (2014) 2858–2868.
[12] P. Gerami, J.P. Alsobrook 2nd, T.J. Palmer, H.S. Robin, Development of a novel noninvasive adhesive patch test for the evaluation of pigmented lesions of the skin, J. Am. Acad. Dermatol. 71 (2014) 237–244.
[13] L. Chang, Z. Hu, Z. Zhou, H. Zhang, Linc00518 contributes to multidrug resistance through regulating the MiR-199a/MRP1 axis in breast cancer, Cell. Physiol. Biochem. 48 (2018) 16–28.
[14] C. Pulito, I. Terrenato, A. Di Benedetto, E. Korita, F. Goeman, A. Sacconi, F. Biagioni, G. Blandino, S. Strano, P. Muti, M. Mottolese, E. Falvo, Cdx2 polymorphism affects the activities of vitamin D receptor in human breast cancer cell lines and human breast carcinomas, PLoS One 10 (2015) e0124894.
[15] H. Sakamoto, T. Asahara, O. Chonan, N. Yuki, H. Mutoh, S. Hayashi, H. Yamamoto, K. Sugano, Comparative analysis of gastrointestinal microbiota between normal and caudal-related homeobox 2 (cdx2) transgenic mice, Intest. Res. 13 (2015) 39–49.
[16] S. He, X.J. Sun, J.B. Zheng, J. Qi, N.Z. Chen, W. Wang, G.B. Wei, D. Liu, J.H. Yu, S.Y. Lu, H. Wang, Recombinant lentivirus with enhanced expression of caudal-related homeobox protein 2 inhibits human colorectal cancer cell proliferation in vitro, Mol. Med. Rep. 12 (2015) 1838–1844.
[17] Q. Xiao, Z. Chen, X. Jin, R. Mao, Z. Chen, The many postures of noncanonical Wnt signaling in development and diseases, Biomed. Pharmacother. 93 (2017) 359–369.
[18] S.G. Pohl, N. Brook, M. Agostino, F. Arfuso, A.P. Kumar, A. Dharmarajan, Wnt signaling in triple-negative breast cancer, Oncogene 6 (2017) e310.
[19] G.B. Jang, J.Y. Kim, S.D. Cho, K.S. Park, J.Y. Jung, H.Y. Lee, I.S. Hong, J.S. Nam, Blockade of Wnt/beta-catenin signaling suppresses breast cancer metastasis by inhibiting CSC-like phenotype, Sci. Rep. 5 (2015) 12465.
[20] B. Nami, Z. Wang, HER2 in breast cancer stemness: a negative feedback loop towards trastuzumab resistance, Cancers (Basel) 9 (2017).
[21] X. Liu, X. Zhang, Q. Zhan, M.V. Brock, J.G. Herman, M. Guo, CDX2 serves as a Wnt signaling inhibitor and is frequently methylated in lung cancer, Cancer Biol. Ther. 13 (2012) 1152–1157.
[22] A.K. Olsen, M. Coskun, M. Bzorek, M.H. Kristensen, E.T. Danielsen, S. Jorgensen, J. Olsen, U. Engel, S. Holck, J.T. Troelsen, Regulation of APC and AXIN2 expression by intestinal tumor suppressor CDX2 in colon cancer cells, Carcinogenesis 34 (2013) 1361–1369.
[23] M.D. Robinson, D.J. McCarthy, G.K. Smyth, edgeR: a Bioconductor package for differential expression analysis of digital gene expression data, Bioinformatics 26 (2010) 139–140.
[24] A. Lebeau, M. Kriegsmann, E. Burandt, H.P. Sinn, Invasive breast cancer: the current WHO classification, Pathologe 35 (2014) 7–17.
[25] M.L. Kwan, R. Haque, V.S. Lee, W.L. Joanie Chung, C.C. Avila, H.A. Clancy, V.P. Quinn, L.H. Kushi, Validation of AJCC TNM staging for breast tumors diagnosed before 2004 in cancer registries, Cancer Causes Control 23 (2012) 1587–1591.
[26] D. Atkins, K.A. Reiffen, C.L. Tegtmeier, H. Winther, M.S. Bonato, S. Storkel, Immunohistochemical detection of EGFR in paraffin-embedded tumor tissues: variation in staining intensity due to choice of fixative and storage time of tissue sections, J. Histochem. Cytochem. 52 (2004) 893–901.
[27] J.J. Lee, J. Geli, C. Larsson, G. Wallin, M. Karimi, J. Zedenius, A. Hoog, T. Foukakis, Gene-specific promoter hypermethylation without global hypomethylation in follicular thyroid cancer, Int. J. Oncol. 33 (2008) 861–869.
[28] S.M. Ayuk, H. Abrahamse, N.N. Houreld, The role of photobiomodulation on gene expression of cell adhesion molecules in diabetic wounded fibroblasts in vitro, J. Photochem. Photobiol. B 161 (2016) 368–374.
[29] I. Dhennin-Duthille, M. Gautier, M. Faouzi, A. Guilbert, M. Brevet, D. Vaudry, A. Ahidouch, H. Sevestre, H. Ouadid-Ahidouch, High expression of transient receptor potential channels in human breast cancer epithelial cells and tissues: correlation with pathological parameters, Cell. Physiol. Biochem. 28 (2011) 813–822.
[30] W. Cheng, H. Fu, F. Feng, C. Ma, J. Li, S. Chen, H. Wang, Efficacy of lentiviral-mediated transfection of hTSHR in poorly differentiated thyroid carcinoma cell line, Nucl. Med. Biol. 40 (2013) 576–580.
[31] A.L. Allan, S.A. Vantyghem, A.B. Tuck, A.F. Chambers, Tumor dormancy and cancer stem cells: implications for the biology and treatment of breast cancer metastasis, Breast Dis. 26 (2006) 87–98.
[32] Z. Jiang, Y. Zhou, K. Devarajan, C.M. Slater, M.B. Daly, X. Chen, Identifying putative breast cancer-associated long intergenic non-coding RNA loci by high density SNP array analysis, Front. Genet. 3 (2012) 299.
[33] Y. Zhang, E.K. Wagner, X. Guo, I. May, Q. Cai, W. Zheng, C. He, J. Long, Long intergenic non-coding RNA expression signature in human breast cancer, Sci. Rep. 6 (2016) 37821.
[34] J. Wang, C. Ye, H. Xiong, Y. Shen, Y. Lu, J. Zhou, L. Wang, Dysregulation of long non-coding RNA in breast cancer: an overview of mechanism and clinical implication, Oncotarget 8 (2017) 5508–5522.
[35] F. Yang, Y.H. Liu, S.Y. Dong, Z.H. Yao, L. Lv, R.M. Ma, X.X. Dai, J. Wang, X.H. Zhang, O.C. Wang, Co-expression networks revealed potential core lncRNAs in the triple-negative breast cancer, Gene 591 (2016) 471–477.
[36] L.K. Ferris, B. Jansen, J. Ho, K.J. Busam, K. Gross, D.D. Hansen, J.P. Alsobrook 2nd, Z. Yao, G.L. Peck, P. Gerami, Utility of a noninvasive 2-gene molecular assay for cutaneous melanoma and effect on the decision to biopsy, JAMA Dermatol. 153 (2017) 675–680.
[37] P. Jonsson, C. Coarfa, F. Mesmar, T. Raz, K. Rajapakshe, J.F. Thompson, P.H. Gunaratne, C. Williams, Single-molecule sequencing reveals estrogen-regulated clinically relevant lncRNAs in breast Cancer, Mol. Endocrinol. 29 (2015) 1634–1645.
[38] T. Liu, X. Zhang, C.K. So, S. Wang, P. Wang, L. Yan, R. Myers, Z. Chen, A.P. Patterson, C.S. Yang, X. Chen, Regulation of Cdx2 expression by promoter methylation, and effects of Cdx2 transfection on morphology and gene expression of human esophageal epithelial cells, Carcinogenesis 28 (2007) 488–496.
[39] P. Rotkrua, Y. Akiyama, Y. Hashimoto, T. Otsubo, Y. Yuasa, MiR-9 downregulates CDX2 expression in gastric cancer cells, Int. J. Cancer 129 (2011) 2611–2620.
[40] G. Jiang, C. Luo, M. Sun, Z. Zhao, W. Li, K. Chen, T. Fan, Methylation of CDX2 as a predictor in poor clinical outcome of patients with colorectal Cancer, Genet. Test. Mol. Biomarkers 20 (2016) 710–714.
[41] Y. Wang, Z. Li, W. Li, S. Liu, B. Han, Methylation of promoter region of CDX2 gene in colorectal cancer, Oncol. Lett. 12 (2016) 3229–3233.
[42] J.B. Zheng, L.N. Qiao, X.J. Sun, J. Qi, H.L. Ren, G.B. Wei, P.H. Zhou, J.F. Yao, L. Zhang, P.B. Jia, Overexpression of caudal-related homeobox transcription factor 2 inhibits the growth of transplanted colorectal tumors in nude mice, Mol. Med. Rep. 12 (2015) 3409–3415.
[43] J. Bondi, G. Bukholm, J.M. Nesland, I.R. Bukholm, Expression of non-membranous beta-catenin and gamma-catenin, c-Myc and cyclin D1 in relation to patient outcome in human colon adenocarcinomas, APMIS 112 (2004) 49–56.
[44] H.M. Kim, C.S. Kim, J.H. Lee, S.J. Jang, J.J. Hwang, S. Ro, J. Choi, CG0009, a novel glycogen synthase kinase 3 inhibitor, induces cell death through cyclin D1 depletion in breast cancer cells, PLoS One 8 (2013) e60383.
[45] Y.S. Deol, M.W. Nasser, L. Yu, X. Zou, R.K. Ganju, Tumor-suppressive effects of psoriasin (S100A7) are mediated through the beta-catenin/T cell factor 4 protein pathway in estrogen receptor-positive breast cancer cells, J. Biol. Chem. 286 (2011) 44845–44854.
[46] Y. Shimomura, D. Agalliu, A. Vonica, V. Luria, M. Wajid, A. Baumer, S. Belli, L. Petukhova, A. Schinzel, A.H. Brivanlou, B.A. Barres, A.M. Christiano, APCDD1 is a novel Wnt inhibitor mutated in hereditary hypotrichosis simplex, Nature 464 (2010) 1043–1047.
[47] M. Rima, M. Daghsni, A. Lopez, Z. Fajloun, L. Lefrancois, M. Dunach, Y. Mori, P. Merle, J.L. Bruses, M. De Waard, M. Ronjat, Down-regulation of the Wnt/beta-catenin signaling pathway by Cacnb4, Mol. Biol. Cell 28 (2017) 3699–3708.
[48] J. He, T. Sheng, A.A. Stelter, C. Li, X. Zhang, M. Sinha, B.A. Luxon, J. Xie, Suppressing Wnt signaling by the hedgehog pathway through sFRP-1, J. Biol. Chem. 281 (2006) 35598–35602.
[49] A.A. Bhat, A. Sharma, J. Pope, M. Krishnan, M.K. Washington, A.B. Singh, P. Dhawan, Caudal homeobox protein Cdx-2 cooperates with Wnt pathway to regulate claudin-1 expression in colon cancer cells, PLoS One 7 (2012) e37174.
[50] C. Toth, F. Sukosd, E. Valicsek, E. Herpel, P. Schirmacher, L. Tiszlavicz, Loss of CDX2 gene expression is associated with DNA repair proteins and is a crucial member of the Wnt signaling pathway in liver metastasis of colorectal cancer, Oncol. Lett. 15 (2018) 3586–3593.
[51] E. Casas, J. Kim, A. Bendesky, L. Ohno-Machado, C.J. Wolfe, J. Yang, Snail2 is an essential mediator of Twist1-induced epithelial mesenchymal transition and metastasis, Cancer Res. 71 (2011) 245–254.
[52] M.H. Jang, H.J. Kim, E.J. Kim, Y.R. Chung, S.Y. Park, Expression of epithelial-mesenchymal transition-related markers in triple-negative breast cancer: ZEB1 as a potential biomarker for poor clinical outcome, Hum. Pathol. 46 (2015) 1267–1274.